Mass spectra of singly heavy baryons in the relativized quark model with heavy-quark dominance*

Zhen-Yu Li (李振宇)[1,4†] Guo-Liang Yu (于国梁)[2‡] Zhi-Gang Wang (王志刚)[2§]
Jian-Zhong Gu (顾建中)[3ǂ] Hong-Tao Shen (沈洪涛)[4♯]

[1]School of Physics and Electronic Science, Guizhou Education University, Guiyang 550018, China
[2]Department of Mathematics and Physics, North China Electric Power University, Baoding 071003, China
[3]China Institute of Atomic Energy, Beijing 102413,China
[4]Guangxi Key Lab of Nuclear Physics and Technology, Guangxi Normal University, Guilin 541006, China

Abstract: The rigorous calculation of the spin-orbit terms in the three-quark system is realized based on the Gaussian expansion method and the infinitesimally-shifted Gaussian basis functions in the framework of the relativized quark model, by ignoring the mixing between different excited states. Then, the complete mass spectra of the singly heavy baryons are obtained rigorously, under the mechanism of the heavy-quark dominance. On these bases, the systematical analyses are carried out for the reliability and predictive power of the model, the fine structure of the singly heavy baryon spectra, the assignments of the excited baryons, and some important topics about the heavy baryon spectroscopy such as the missing states, the 'spin-orbit puzzle', the clustering effect, etc. The result confirms that under the heavy-quark dominance mechanism, the relativized quark model can describe the excitation spectra and the fine structures of the singly heavy baryons correctly and precisely.

Keywords: Singly heavy baryon, Spin-orbit interactions, Heavy-quark dominance, Fine structure, Relativized quark model

DOI: **CSTR:** 32044.14.ChinesePhysicsC.

I. INTRODUCTION

The heavy baryon spectroscopy is crucial for gaining deeper insights into the strong interaction in the non-perturbative regime of the Quantum Chromodynamics (QCD) [1]. It has attracted considerable experimental and theoretical attentions. So far, a large number of singly heavy baryons have been observed in experiment [2–22], which provides an important support for related theoretical researches [23–25].

In the new Review of Particle Physics (RPP) by the Particle Data Group (PDG), more than 70 singly heavy baryons have been collected [2]. These heavy baryons and their J^P values are listed in Table 1, which shows that most of the ground states of the heavy baryons have been well established in experiment. But the J^P values of many excited baryons have not been identified. Moreover, some of the excited baryons were observed experimentally in groups, and their mass values are very close to each other, such as $\{\Omega_c^0(3000)$, $\Omega_c^0(3050)$, $\Omega_c^0(3065)$, $\Omega_c^0(3090)$, $\Omega_c^0(3120)\}$, $\{\Xi_c(2923)^0$, $\Xi_c(2930)^{+,0}$, $\Xi_c(2970)^{+,0}\}$, and $\{\Omega_b(6316)^-$, $\Omega_b(6330)^-$, $\Omega_b(6340)^-$, $\Omega_b(6350)^-\}$. These close mass values in each group indicate a fine structure in their excitation spectra, which is, however, an unsolved problem in the current theory. In addition, lots of the excited heavy baryons as shown in Table 1 have been observed in the last few years, due to the improvement of experimental accuracy by some collaborations such as the LHCb, the Belle, the CMS, etc. Very recently, a new charmed baryon $\Xi_c(2923)^+$ was

Received 21 May 2025; Accepted 15 July 2025

* This research was supported by the Open Project of Guangxi Key Lab of Nuclear Physics and Technology (No. NLK2023-04), the Central Government Guidance Funds for Local Scientific and Technological Development in China (No. Guike ZY22096024), the Natural Science Foundation of Guizhou Province-ZK[2024](General Project)650, the National Natural Science Foundation of China (Grant Nos. 11675265, 12175068), the Continuous Basic Scientific Research Project (Grant No. WD-JC-2019-13) and the Leading Innovation Project (Grant No. LC 192209000701)

† E-mail: zhenyvli@163.com
‡ E-mail: yuguoliang2011@163.com
§ E-mail: zgwang@aliyun.com
ǂ E-mail: gujianzhong2000@aliyun.com
♯ E-mail: shenht@gxnu.edu.cn

Table 1. Observed singly heavy baryons and their J^P values [2]. The $\Sigma_c(2846)^0$ and the $\Xi_c(2923)^+$ are cited from Ref. [5] and Ref. [22], respectively.

Baryon	J^P	Baryon	J^P	Baryon	J^P	Baryon	J^P	Baryon	J^P	Baryon	J^P	Baryon	J^P	Baryon	J^P
Λ_c^+	$\frac{1}{2}^+$	$\Sigma_c(2455)^{++}$	$\frac{1}{2}^+$	Ξ_c^+	$\frac{1}{2}^+$	Ω_c^0	$\frac{1}{2}^+$	Λ_b^0	$\frac{1}{2}^+$	Σ_b^+	$\frac{1}{2}^+$	Ξ_b^0	$\frac{1}{2}^+$	Ω_b^-	$\frac{1}{-}^+$
$\Lambda_c(2595)^+$	$\frac{1}{2}^-$	$\Sigma_c(2455)^+$	$\frac{1}{2}^+$	Ξ_c^0	$\frac{1}{2}^+$	$\Omega_c(2770)^0$	$\frac{3}{2}^+$	$\Lambda_b(5912)^0$	$\frac{1}{2}^-$	Σ_b^-	$\frac{1}{2}^+$	Ξ_b^-	$\frac{1}{2}^+$	$\Omega_b(6316)^-$	$?^?$
$\Lambda_c(2625)^+$	$\frac{3}{2}^-$	$\Sigma_c(2455)^0$	$\frac{1}{2}^+$	$\Xi_c'^+$	$\frac{1}{2}^+$	$\Omega_c(3000)^0$	$?^?$	$\Lambda_b(5920)^0$	$\frac{3}{2}^-$	Σ_b^{*+}	$\frac{3}{2}^+$	$\Xi_b(5935)^-$	$\frac{1}{2}^+$	$\Omega_b(6330)^-$	$?^?$
$\Lambda_c(2765)^+$	$?^?$	$\Sigma_c(2520)^{++}$	$\frac{3}{2}^+$	$\Xi_c'^0$	$\frac{1}{2}^+$	$\Omega_c(3050)^0$	$?^?$	$\Lambda_b(6070)^0$	$\frac{1}{2}^+$	Σ_b^{*-}	$\frac{3}{2}^+$	$\Xi_b(5945)^0$	$\frac{3}{2}^+$	$\Omega_b(6340)^-$	$?^?$
$\Lambda_c(2860)^+$	$\frac{3}{2}^+$	$\Sigma_c(2520)^+$	$\frac{3}{2}^+$	$\Xi_c(2645)^+$	$\frac{3}{2}^+$	$\Omega_c(3065)^0$	$?^?$	$\Lambda_b(6146)^0$	$\frac{3}{2}^+$	$\Sigma_b(6097)^+$	$?^?$	$\Xi_b(5955)^-$	$\frac{3}{2}^+$	$\Omega_b(6350)^-$	$?^?$
$\Lambda_c(2880)^+$	$\frac{5}{2}^+$	$\Sigma_c(2520)^0$	$\frac{3}{2}^+$	$\Xi_c(2645)^0$	$\frac{3}{2}^+$	$\Omega_c(3090)^0$	$?^?$	$\Lambda_b(6152)^0$	$\frac{5}{2}^+$	$\Sigma_b(6097)^-$	$?^?$	$\Xi_b(6087)^0$	$\frac{3}{2}^-$		
$\Lambda_c(2910)^+$	$?^?$	$\Sigma_c(2800)^{++}$	$?^?$	$\Xi_c(2790)^+$	$\frac{1}{2}^-$	$\Omega_c(3120)^0$	$?^?$					$\Xi_b(6095)^0$	$\frac{3}{2}^-$		
$\Lambda_c(2940)^+$	$\frac{3}{2}^-$	$\Sigma_c(2800)^+$	$?^?$	$\Xi_c(2790)^0$	$\frac{1}{2}^-$	$\Omega_c(3185)^0$	$?^?$					$\Xi_b(6100)^-$	$\frac{3}{2}^-$		
		$\Sigma_c(2800)^0$	$?^?$	$\Xi_c(2815)^+$	$\frac{3}{2}^-$	$\Omega_c(3327)^0$	$?^?$					$\Xi_b(6227)^0$	$?^?$		
		$\Sigma_c(2846)^0$	$?^?$	$\Xi_c(2815)^0$	$\frac{3}{2}^-$							$\Xi_b(6227)^-$	$?^?$		
				$\Xi_c(2882)^0$	$?^?$							$\Xi_b(6327)^0$	$?^?$		
				$\Xi_c(2923)^+$	$?^?$							$\Xi_b(6333)^0$	$?^?$		
				$\Xi_c(2923)^0$	$?^?$										
				$\Xi_c(2930)^+$	$?^?$										
				$\Xi_c(2930)^0$	$?^?$										
				$\Xi_c(2970)^+$	$\frac{1}{2}^+$										
				$\Xi_c(2970)^0$	$\frac{1}{2}^+$										
				$\Xi_c(3055)^+$	$?^?$										
				$\Xi_c(3080)^+$	$?^?$										
				$\Xi_c(3080)^0$	$?^?$										
				$\Xi_c(3120)^+$	$?^?$										

firstly observed by the LHCb collaboration [22]. It is expected that more heavy baryons will be observed in the near future, and more fine structures are also expected to be discovered.

All these experimental progresses show that it is time to systematically analyze the data and delineate a reliable mass spectrum. However, it is not a simple matter to give an accurate analysis of these observed heavy baryons theoretically, which has actually become a great challenge for various theoretical methods. As an indispensable tool for understanding of the multitude of observed baryons and their properties, the relativized quark model with QCD also faces the same challenge.

The relativized quark model was developed by Godfrey and Isgur in 1985 [26], and has achieved great success in analyzing the meson spectra. The Hamiltonian of this model is based on a universal one-gluon-exchange-plus-linear-confinement potential motivated by QCD, which contains almost all possible forms of the main interaction between the two quarks. In 1986, Capstick and Isgur extended this model and insisted on using the method of studying light-quark baryons and systematically studied the mass spectra of both light and heavy baryons under a unified framework [27]. Their study in the baryon spectroscopy produced a lasting effect [28]. However, their study predicted more 'missing' states of the heavy baryons, which is very similar to the case of the light-quark baryons. Once more, in a similar manner to the light-quark baryons, there are two possible solutions to the problem for the heavy baryons summarized by Capstick and Roberts. The first one is that the dynamical degrees of freedom used in the model, namely the three valence quarks, are not physically realized. Instead, a baryon consists of a quark and a diquark, and the reduction of the number of internal degrees of freedom leads to a more sparsely populated spectrum. The second possible solution is that the missing states couple weakly to the formation channels used to investigate the states, and so

give very small contributions to the scattering cross sections [29].

Later, the heavy quark symmetry [30], the heavy quark limit [31] and the heavy quark effective theory [32, 33] were put forward one after another, and revealed some important structure properties of the heavy baryons, which laid the foundation for the solution of the above problem. According to the first possible solution, Ebert, Faustov and Galkin analyzed the spectra of the singly heavy baryons in the heavy quark-light diquark picture [34], and predicted significantly fewer states than those of Ref. [27] mentioned above, which has two important implications. One is that the total orbital angular momentum L can be approximatively regarded as a good quantum number of a baryon state, even though it is not true strictly in a relativistic theory. In practice, as an approximative good quantum number, L has been widely used in researches [35–43]. An other is that the concept of 'the clustering effect' is officially applied in study, which means there might exist the cluster in the singly heavy baryon, if this solution is correct. However, the reliability of the first solution has yet to be tested further. 'It is telling that this simple diagnostic is difficult to apply since so little is known of the excited baryon spectrum' [1].

Inspired by the above related theoretical works, we studied the spectra of the singly and doubly heavy baryons systematically in the framework of the relativized quark model [44–48]. The used method adopted the respective advantages of the above two possible solutions. We considered L to be an approximative good quantum number, assumed the stable (or physically realized) quantum states for the excited heavy baryons should live in the lower orbital excitation mode, and further ignored the mixing between different excited states. The results showed that most of the experimental data can be well described with a uniform set of parameters for the heavy baryons. We analyzed the orbital excitation of the heavy baryons carefully and proposed the heavy-quark dominance (HQD) mechanism, which may solve the problem of the 'missing' states in a natural way, and determine the overall structure of the excitation spectra for the singly and doubly heavy baryons [49].

For describing the fine structure of the observed excited baryons, we improved the calculation of the spin-orbit interactions by considering the contribution from the light-quark cluster in a quasi-two-body spin-orbit interaction, which enhances the energy level splitting of the orbital excitation significantly and presents a reasonable fine structure [50]. The analysis of the fine structure confirms that the contribution of the spin-orbit interaction from the orbital angular momentum $\mathbf{l}_\lambda$ is not negligible.

The predicted singly heavy baryon spectra in our works match well with the current data. But, it is still unsatisfactory because the approximate formulas were used for describing the contributions of the spin-orbit interaction to the fine structures [50], as a result, one cannot judge the deviation from the real results. This reduces the reliability of the calculation and the predictive power. So, it is necessary to analyze the fine structure by using the rigorous calculation. However, the rigorous calculation is a common tough problem in the three-body systems. Because the Hamiltonian of the relativized quark model is based on the two-body interaction, one will encounter some technical difficulties in the rigorous calculation, when the model is extended from the mesons to the baryons. This is indeed the biggest obstacle that this model has encountered in studying the three-quark systems. If the rigorous calculation is implemented, some important problems of this model appearing in the heavy baryon spectroscopy might be solved, such as the missing states [29], the 'spin-orbit puzzle' [51, 52], the clustering effect in a heavy baryon, etc. And a more important question could also be answered, i.e., whether and how the relativized quark model can correctly describe the heavy baryon spectroscopy.

In this work, we will try to perform the rigorous calculation of the heavy baryon spectra in the relativized quark model with the HQD mechanism, by using the Gaussian expansion method (GEM) and the infinitesimally-shifted Gaussian (ISG) basis functions [53, 54], so as to obtain a complete mass spectrum of the singly heavy baryons, answer the questions mentioned above and provide a reliable analysis for the relative researches.

The remainder of this paper is organized as follows. In Sec. II, the theoretical methods used in this work are introduced, including the Hamiltonian of the relativized quark model, the wave functions and the Jacobi coordinates, and the evaluations of the matrix elements, including the rigorous calculation of the spin-orbit terms. The structure properties of the singly heavy baryon spectra, the comparison between the calculated excitation spectra and the experimental data, and the reliability of the model are analyzed in Sec. III. And Sec. IV is reserved for the conclusions.

II. THEORETICAL METHODS USED IN THIS WORK

A. Hamiltonian of the relativized quark model

In the relativized quark model, the Hamiltonian for a three-quark system is based on the two-body interactions,

$$\begin{aligned} H &= H_0 + \tilde{H}^{conf} + \tilde{H}^{hyp} + \tilde{H}^{so} \\ &= \sum_{i=1}^{3} \sqrt{p_i^2 + m_i^2} + \sum_{i<j} (\tilde{H}_{ij}^{conf} + \tilde{H}_{ij}^{hyp} + \tilde{H}_{ij}^{so}), \end{aligned} \tag{1}$$

where the interaction terms $\tilde{H}_{ij}^{conf}$, $\tilde{H}_{ij}^{hyp}$ and $\tilde{H}_{ij}^{so}$ are the

confinement, hyperfine and spin-orbit interactions, respectively. The confinement term $\tilde{H}_{ij}^{conf}$ includes a modified one-gluon-exchange potential $G'_{ij}(r)$ and a smeared linear confinement potential $\tilde{S}_{ij}(r)$. The hyperfine interaction $\tilde{H}_{ij}^{hyp}$ consists of the tensor term $\tilde{H}_{ij}^{tensor}$ and the contact term $\tilde{H}_{ij}^{c}$. And the spin-orbit interaction $\tilde{H}_{ij}^{so}$ can be divided into the color-magnetic term $\tilde{H}_{ij}^{so(v)}$ and the Thomas-precession term $\tilde{H}_{ij}^{so(s)}$. Their forms are described in detail below.

$$\begin{aligned}\tilde{H}_{ij}^{conf} &= G'_{ij}(r)+\tilde{S}_{ij}(r),\\ \tilde{H}_{ij}^{hyp} &= \tilde{H}_{ij}^{tensor}+\tilde{H}_{ij}^{c},\\ \tilde{H}_{ij}^{so} &= \tilde{H}_{ij}^{so(v)}+\tilde{H}_{ij}^{so(s)},\end{aligned} \tag{2}$$

with

$$\begin{aligned}\tilde{H}_{ij}^{tensor} = &-\frac{\mathbf{s}_i\cdot\mathbf{r}_{ij}\mathbf{s}_j\cdot\mathbf{r}_{ij}/r_{ij}^2-\frac{1}{3}\mathbf{s}_i\cdot\mathbf{s}_j}{m_i m_j}\\ &\times\left(\frac{\partial^2}{\partial r_{ij}^2}-\frac{1}{r_{ij}}\frac{\partial}{\partial r_{ij}}\right)\tilde{G}_{ij}^{t},\end{aligned} \tag{3}$$

$$\tilde{H}_{ij}^{c} = \frac{2\mathbf{s}_i\cdot\mathbf{s}_j}{3m_i m_j}\nabla^2\tilde{G}_{ij}^{c}, \tag{4}$$

$$\begin{aligned}\tilde{H}_{ij}^{so(v)} = &\frac{\mathbf{s}_i\cdot\mathbf{L}_{(ij)i}}{2m_i^2 r_{ij}}\frac{\partial\tilde{G}_{ii}^{so(v)}}{\partial r_{ij}}+\frac{\mathbf{s}_j\cdot\mathbf{L}_{(ij)j}}{2m_j^2 r_{ij}}\frac{\partial\tilde{G}_{jj}^{so(v)}}{\partial r_{ij}}\\ &+\frac{(\mathbf{s}_i\cdot\mathbf{L}_{(ij)j}+\mathbf{s}_j\cdot\mathbf{L}_{(ij)i})}{m_i m_j r_{ij}}\frac{\partial\tilde{G}_{ij}^{so(v)}}{\partial r_{ij}},\end{aligned} \tag{5}$$

$$\tilde{H}_{ij}^{so(s)} = -\frac{\mathbf{s}_i\cdot\mathbf{L}_{(ij)i}}{2m_i^2 r_{ij}}\frac{\partial\tilde{S}_{ii}^{so(s)}}{\partial r_{ij}}-\frac{\mathbf{s}_j\cdot\mathbf{L}_{(ij)j}}{2m_j^2 r_{ij}}\frac{\partial\tilde{S}_{jj}^{so(s)}}{\partial r_{ij}}. \tag{6}$$

Here, the following conventions are used, i.e., $\mathbf{L}_{(ij)i}=\mathbf{r}_{ij}\times\mathbf{p}_i$ and $\mathbf{L}_{(ij)j}=-\mathbf{r}_{ij}\times\mathbf{p}_j$. In the formulas above, G'_{ij}, $\tilde{G}_{ij}^{t}$, $\tilde{G}_{ij}^{c}$, $\tilde{G}_{ij}^{so(v)}$ and $\tilde{S}_{ii}^{so(s)}$ should be modified with the momentum-dependent factors as follows,

$$\begin{aligned}G'_{ij} &= \left(1+\frac{p_{ij}^2}{E_i E_j}\right)^{\frac{1}{2}}\tilde{G}_{ij}(r_{ij})\left(1+\frac{p_{ij}^2}{E_i E_j}\right)^{\frac{1}{2}},\\ \tilde{G}_{ij}^{t} &= \left(\frac{m_i m_j}{E_i E_j}\right)^{\frac{1}{2}+\epsilon_t}\tilde{G}_{ij}(r_{ij})\left(\frac{m_i m_j}{E_i E_j}\right)^{\frac{1}{2}+\epsilon_t},\\ \tilde{G}_{ij}^{c} &= \left(\frac{m_i m_j}{E_i E_j}\right)^{\frac{1}{2}+\epsilon_c}\tilde{G}_{ij}(r_{ij})\left(\frac{m_i m_j}{E_i E_j}\right)^{\frac{1}{2}+\epsilon_c},\\ \tilde{G}_{ij}^{so(v)} &= \left(\frac{m_i m_j}{E_i E_j}\right)^{\frac{1}{2}+\epsilon_{so(v)}}\tilde{G}_{ij}(r_{ij})\left(\frac{m_i m_j}{E_i E_j}\right)^{\frac{1}{2}+\epsilon_{so(v)}},\\ \tilde{S}_{ii}^{so(s)} &= \left(\frac{m_i m_i}{E_i E_i}\right)^{\frac{1}{2}+\epsilon_{so(s)}}\tilde{S}_{ij}(r_{ij})\left(\frac{m_i m_i}{E_i E_i}\right)^{\frac{1}{2}+\epsilon_{so(s)}},\end{aligned} \tag{7}$$

where $E_i=\sqrt{m_i^2+p_{ij}^2}$ is the relativistic kinetic energy, and p_{ij} is the momentum magnitude of either of the quarks in the center-of-mass frame of the ij quark subsystem [27, 55].

$\tilde{G}_{ij}(r_{ij})$ and $\tilde{S}_{ij}(r_{ij})$ are obtained by the smearing transformations of the one-gluon exchange potential $G(r)=-\frac{4\alpha_s(r)}{3r}$ and linear confinement potential $S(r)=\tilde{b}r+\tilde{c}$, respectively,

$$\tilde{G}_{ij}(r_{ij}) = \mathbf{F}_i\cdot\mathbf{F}_j\sum_{k=1}^{3}\frac{2\alpha_k}{\sqrt{\pi}r_{ij}}\int_0^{\tau_{kij}r_{ij}}e^{-x^2}\mathrm{d}x, \tag{8}$$

$$\begin{aligned}\tilde{S}_{ij}(r_{ij}) = &-\frac{3}{4}\mathbf{F}_i\cdot\mathbf{F}_j\{\tilde{b}r_{ij}[\frac{e^{-\sigma_{ij}^2 r_{ij}^2}}{\sqrt{\pi}\sigma_{ij}r_{ij}}\\ &+\left(1+\frac{1}{2\sigma_{ij}^2 r_{ij}^2}\right)\frac{2}{\sqrt{\pi}}\int_0^{\sigma_{ij}r_{ij}}e^{-x^2}\mathrm{d}x]+\tilde{c}\},\end{aligned} \tag{9}$$

with

$$\begin{aligned}\tau_{kij} &= \frac{1}{\sqrt{\frac{1}{\sigma_{ij}^2}+\frac{1}{\gamma_k^2}}},\\ \sigma_{ij} &= \sqrt{s_0^2\left(\frac{2m_i m_j}{m_i+m_j}\right)^2+\sigma_0^2\left[\frac{1}{2}\left(\frac{4m_i m_j}{(m_i+m_j)^2}\right)^4+\frac{1}{2}\right]}.\end{aligned} \tag{10}$$

Here α_k and γ_k are constants. $\mathbf{F}_i\cdot\mathbf{F}_j$ stands for the inner product of the color matrices of quarks i and j. For the baryon, $\langle\mathbf{F}_i\cdot\mathbf{F}_j\rangle=-2/3$. All of the parameters in these formulas are completely consistent with those in our previous works [44, 45]. Their values are listed in Table 2.

B. Wave functions and Jacobi coordinates

For a singly heavy baryon system, the heavy-quark is decoupled from the two light-quarks in the heavy quark limit. With the requirement of the flavor $SU(3)$ subgroups for the light-quark pair, the singly heavy baryons belong to either a sextet ($\mathbf{6}_F$) of the flavor symmetric states,

$$\begin{aligned}&\Sigma_Q=(uu)Q,\ \frac{1}{\sqrt{2}}(ud+du)Q,\ (dd)Q,\\ &\Xi'_Q=\frac{1}{\sqrt{2}}(us+su)Q,\ \frac{1}{\sqrt{2}}(ds+sd)Q,\\ &\Omega_Q=(ss)Q,\end{aligned} \tag{11}$$

or an anti-triplet ($\bar{\mathbf{3}}_F$) of the flavor antisymmetric states [33],

Table 2. Parameters of the relativized quark model in this work. Their values are the same as those in Ref. [26], apart from $\tilde{b}$ and $\tilde{c}$ [44].

m_u/m_d(GeV)	m_s(GeV)	m_c(GeV)	m_b(GeV)	γ_1(GeV)	γ_2(GeV)	γ_3(GeV)	$\tilde{b}$(GeV^2)	$\tilde{c}$(GeV)
0.22	0.419	1.628	4.977	1/2	$\sqrt{10}/2$	$\sqrt{1000}/2$	**0.14**	**−0.198**
ϵ_c	ϵ_t	$\epsilon_{SO(v)}$	$\epsilon_{SO(s)}$	α_1	α_2	α_3	σ_0(GeV)	$\tilde{s}$
−0.168	0.025	−0.035	0.055	0.25	0.15	0.20	1.8	1.55

$$\Lambda_Q = \frac{1}{\sqrt{2}}(ud-du)Q,$$
$$\Xi_Q = \frac{1}{\sqrt{2}}(us-su)Q,\ \frac{1}{\sqrt{2}}(ds-sd)Q. \tag{12}$$

Here u, d and s denote up, down and strange quarks, respectively. Q denotes charm (c) quark or bottom (b) quark.

For describing the internal orbital motion of the singly heavy baryon, we select the specific Jacobi coordinates (named JC-3 for short) as shown in Fig. 1, which is consistent with the above reservation about the flavor wave function naturally. In this work, the Jacobi coordinates are defined as

$$\begin{aligned}\boldsymbol{\rho}_i &= \mathbf{r}_{jk} = \mathbf{r}_j - \mathbf{r}_k,\\ \boldsymbol{\lambda}_i &= \mathbf{r}_i - \frac{m_j\mathbf{r}_j + m_k\mathbf{r}_k}{m_j+m_k},\\ \boldsymbol{R}_i &= \frac{m_i\mathbf{r}_i + m_j\mathbf{r}_j + m_k\mathbf{r}_k}{m_i+m_j+m_k} \equiv \mathbf{0},\end{aligned} \tag{13}$$

where $\{i, j, k\} = \{1, 2, 3\}$, $\{2, 3, 1\}$ or $\{3, 1, 2\}$. $\mathbf{r}_i$ and m_i denote the position vector and the mass of the ith quark, respectively. $\mathbf{R}_i \equiv \mathbf{0}$ means that the kinetic energy of the center of mass is not considered. Specially, for the JC-3 in Fig. 1, the following definitions are used in this work, $\boldsymbol{\rho}_3 \equiv \boldsymbol{\rho}$ and $\boldsymbol{\lambda}_3 \equiv \boldsymbol{\lambda}$.

Based on the above discussion and the heavy quark effective theory (HQET) [31–33], the spin and orbital wave function of a baryon state is assumed to have the coupling scheme

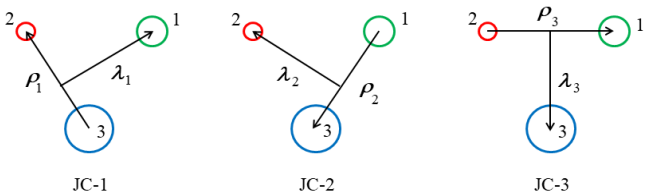

Fig. 1. (color online) There are 3 channels of the Jacobi coordinates for a three-quark system, labeled with $\{\boldsymbol{\rho}_k, \boldsymbol{\lambda}_k\}$ (k=1, 2, 3). The channel 3 (JC-3) is selected for defining the wave function of a singly heavy baryon state. All the quarks are numbered for ease of use in calculations, and the 3rd quark refers specifically to the heavy quark.

$$|(J^P)_j, L\rangle = |\{[(l_\rho l_\lambda)_L(s_1 s_2)_{s_{12}}]_j s_3\}_J\rangle, \tag{14}$$

with $P = (-1)^{l_\rho+l_\lambda}$. $l_\rho(l_\lambda)$, L and s_{12} are the quantum numbers of the relative orbital angular momentum $\mathbf{l}_\rho$ ($\mathbf{l}_\lambda$), total orbital angular momentum $\mathbf{L}$, and total spin of the light-quark pair $\mathbf{s}_{12}$, respectively. j denotes the quantum number of the coupled angular momentum of $\mathbf{L}$ and $\mathbf{s}_{12}$, so that the total angular momentum $J = j \pm \frac{1}{2}$. More precisely, the baryon state is labeled with $(l_\rho, l_\lambda)nL(J^P)_j$, in which n is the quantum number of the radial excitation. It shows that such labeling of quantum states is acceptable, especially, L being approximated as a good quantum number [49]. For the Σ_Q, Ξ_Q' and Ω_Q baryon families, $(-1)^{l_\rho+s_{12}} = -1$ should be also guaranteed due to the total antisymmetry of the wave function of the two light quarks, but $(-1)^{l_\rho+s_{12}} = 1$ for the Λ_Q and Ξ_Q families. All the conventions are based on the JC-3 in Fig. 1.

C. Evaluations of the matrix elements

Since the orbital excited state $|\{[(l_\rho l_\lambda)_L(s_1 s_2)_{s_{12}}]_j s_3\}_J\rangle \equiv |\alpha\rangle_3$ is defined in the JC-3 as discussed above, the matrix elements of the Hamiltonian should be evaluated with the wave function $|\alpha\rangle_3$ of the Jacobi coordinates ($\boldsymbol{\rho}_3$, $\boldsymbol{\lambda}_3$). Here, the subscript 3 stands for JC-3. For a given orbital excited state $|\alpha\rangle_3$, the set of Gaussian basis functions $\{|(\tilde{n},\alpha)_3^G\rangle\}$ form a set of finite-dimensional, non-orthogonal, and complete bases in a finite coordinate (radial) space, which are used in this work to achieve the high precision calculations of the matrix elements. This is the so-call Gaussian expansion method (GEM) [54]. For the evaluation of the matrix element $\langle(\tilde{n},\alpha)_3^G|\hat{H}_{ij}|(\tilde{n}',\alpha)_3^G\rangle$ with $\hat{H}_{ij}(r_{ij}) = \hat{H}(\rho_k)$ (k=1, 2, 3 corresponds to JC-1, -2, -3, respectively), the Jacobi coordinates transformation needs to be performed as $\{\boldsymbol{\rho}_3, \boldsymbol{\lambda}_3\} \to \{\boldsymbol{\rho}_k, \boldsymbol{\lambda}_k\}$. However, it will be very tedious in the framework of the GEM.

This laborious process can be simplified by introducing the infinitesimally-shifted Gaussian (ISG) basis functions [54]. With the help of the ISG basis functions, the matrix elements of the Hamiltonian terms H_0, G'_{ij}, $\tilde{S}_{ij}$, $\tilde{H}_{ij}^{tensor}$, and $\tilde{H}_{ij}^{c}$ can be evaluated rigorously in our previous works. The GEM and ISG basis functions are briefly introduced in Appendix A and Appendix B, respectively. The detailed results can be found in Ref. [44].

In this work, the rigorous calculation of the spin-orbit

terms $\langle(\tilde{n},\alpha)^G_3|\tilde{H}^{SO}_{ij}|(\tilde{n}',\alpha)^G_3\rangle$ is realized in the framework of the GEM and the ISG basis functions, by ignoring the mixing between different excited states. The detailed analysis is presented in Appendix C.

Now, all of the Hamiltonian matrix elements are evaluated. The eigenvalues of the Hamiltonian can be obtained rigorously, for the orbital excited states and their radial excited states.

III. RESULTS AND DISCUSSIONS

For the L-wave excitation with $\mathbf{L}=\mathbf{l}_\rho+\mathbf{l}_\lambda$, there are an infinite number of orbital excitation modes. Taking $L=1$ as an example, the excitation modes $(l_\rho,l_\lambda)_L$ are $(1,0)_1$, $(0,1)_1$, $(1,1)_1$, $(2,1)_1$, $(1,2)_1$, $(2,2)_1$, and so on. We assume that the excitation mode with the lowest energy level is the most stable and has the greatest probability of being observed experimentally, which dominates the structure of the excitation spectrum. This assumption is summarized as the HQD approximation (or the HQD mechanism) [49].

In the HQD mechanism, the orbital excited states of the singly heavy baryons mainly come from the λ-modes $(l_\rho=0,l_\lambda)_{L=l_\lambda}$. But for the P-wave orbital excitations of the charm baryons with the $\mathbf{6}_F$ sector, i.e., the Σ_c, Ξ'_c and Ω_c families, the HQD mechanism is broken because the mass of c quark is not heavy enough, where both the λ-mode $(0,1)_1$ and the ρ-mode $(1,0)_1$ appear in their P-wave states.

Based on the above analyses, the S-, P- and D-wave

Table 3. Contribution of each Hamiltonian term to the mass values (in MeV) for the $1S$-, $1P$- and $1D$-wave states of the Λ_c and Σ_c baryons with $\langle H_{mode}\rangle \equiv \langle H_0+H^{conf}\rangle$ and $\langle H_{ij}\rangle \equiv \langle H\rangle - \langle (H-H_{ij})\rangle$. The orbital excited states of the ρ-mode are marked in bold type.

$(l_\rho,l_\lambda)nL(J^P)_j$	$\langle H_{mode}\rangle$	$\{\langle H^t_{12}\rangle$	$\langle H^t_{23}\rangle$	$\langle H^t_{31}\rangle\}$	$\{\langle H^c_{12}\rangle$	$\langle H^c_{23}\rangle$	$\langle H^c_{31}\rangle\}$	$\{\langle H^{SO(v)}_{12}\rangle$	$\langle H^{SO(v)}_{23}\rangle$	$\langle H^{SO(v)}_{31}\rangle\}$	$\{\langle H^{SO(s)}_{12}\rangle$	$\langle H^{SO(s)}_{23}\rangle$	$\langle H^{SO(s)}_{31}\rangle\}$	$\langle H\rangle$
							Λ_c							
$(0,0)1S(\frac{1}{2}^+)_0$	2464.30	{ 0	0	0 }	{ −176.49	0	0 }	{ 0	0	0 }	{ 0	0	0 }	2287.81
$(0,1)1P(\frac{1}{2}^-)_1$	2781.78	{ 0	0	0 }	{ −162.80	0	0 }	{ 0	−15.52	−15.52 }	{ 0	3.84	3.84 }	2596.87
$(0,1)1P(\frac{3}{2}^-)_1$	2781.78	{ 0	0	0 }	{ −161.42	0	0 }	{ 0	7.32	7.32 }	{ 0	−1.86	−1.86 }	2630.92
$(0,2)1D(\frac{3}{2}^+)_2$	3041.20	{ 0	0	0 }	{ −156.64	0	0 }	{ 0	−10.51	−10.51 }	{ 0	4.40	4.40 }	2872.53
$(0,2)1D(\frac{5}{2}^+)_2$	3041.20	{ 0	0	0 }	{ −156.61	0	0 }	{ 0	6.61	6.61 }	{ 0	−2.86	−2.86 }	2892.15
							Σ_c							
$(0,0)1S(\frac{1}{2}^+)_1$	2464.30	{ 0	0	0 }	{ 48.04	−27.58	−27.58 }	{ 0	0	0 }	{ 0	0	0 }	2456.24
$(0,0)1S(\frac{3}{2}^+)_1$	2464.30	{ 0	0	0 }	{ 44.24	11.93	11.93 }	{ 0	0	0 }	{ 0	0	0 }	2533.92
$(0,1)1P(\frac{1}{2}^-)_0$	2781.78	{ 0	0	0 }	{ 42.06	0	0 }	{ 0	−43.18	−43.18 }	{ 0	17.15	17.15 }	2773.06
$(0,1)1P(\frac{1}{2}^-)_1$	2781.78	{ 0	0	0 }	{ 41.80	−4.72	−4.72 }	{ 0	−29.27	−29.27 }	{ 0	10.53	10.53 }	2778.02
$(0,1)1P(\frac{3}{2}^-)_1$	2781.78	{ 0	0.74	0.74 }	{ 41.13	2.14	2.14 }	{ 0	−16.78	−16.78 }	{ 0	7.79	7.79 }	2810.40
$(0,1)1P(\frac{3}{2}^-)_2$	2781.78	{ 0	−0.44	−0.44 }	{ 40.65	−6.02	−6.02 }	{ 0	9.38	9.38 }	{ 0	−6.02	−6.02 }	2816.13
$(\mathbf{1},\mathbf{0})1P(\frac{1}{2}^-)_1$	2874.52	{ 0	0	0 }	{ −13.81	0	0 }	{ 0	−16.64	−16.64 }	{ 0	0	0 }	**2828.13**
$(0,1)1P(\frac{5}{2}^-)_2$	2781.78	{ 0	1.38	1.38 }	{ 39.79	3.38	3.38 }	{ 0	25.01	25.01 }	{ 0	−10.68	−10.68 }	2862.97
$(\mathbf{1},\mathbf{0})1P(\frac{3}{2}^-)_1$	2874.52	{ 0	0	0 }	{ −13.11	0	0 }	{ 0	8.07	8.07 }	{ 0	0	0 }	**2877.37**
$(0,2)1D(\frac{1}{2}^+)_1$	3041.20	{ 0	0	0 }	{ 39.77	1.72	1.72 }	{ 0	−42.03	−42.03 }	{ 0	23.07	23.07 }	3048.14
$(0,2)1D(\frac{3}{2}^+)_1$	3041.20	{ 0	−0.73	−0.73 }	{ 39.72	−0.79	−0.79 }	{ 0	−24.37	−24.37 }	{ 0	16.41	16.41 }	3062.98
$(0,2)1D(\frac{3}{2}^+)_2$	3041.20	{ 0	−0.14	−0.14 }	{ 39.28	−0.76	−0.76 }	{ 0	−18.78	−18.78 }	{ 0	9.95	9.95 }	3061.57
$(0,2)1D(\frac{5}{2}^+)_2$	3041.20	{ 0	0.46	0.46 }	{ 39.22	0.44	0.44 }	{ 0	−3.66	−3.66 }	{ 0	3.90	3.90 }	3082.51
$(0,2)1D(\frac{5}{2}^+)_3$	3041.20	{ 0	−0.64	−0.64 }	{ 38.59	−1.65	−1.65 }	{ 0	9.43	9.43 }	{ 0	−8.91	−8.91 }	3076.68
$(0,2)1D(\frac{7}{2}^+)_3$	3041.20	{ 0	1.29	1.29 }	{ 38.53	1.05	1.05 }	{ 0	23.17	23.17 }	{ 0	−15.54	−15.54 }	3101.93

states together with their radial excitations of the singly heavy baryons are investigated systematically, and the complete mass spectra are obtained. Taking the Λ_c and the Σ_c as examples, the contribution of each Hamiltonian term to the energy levels is given in Table 3 of Appendix D, so as to figure out the energy level splitting, the energy level evolution with each Hamiltonian term, and the formation of the fine structures. For the low-lying states, i.e., the $1S$-, $2S$-, $3S$-, $1P$-, $2P$- (only for the $\bar{\mathbf{3}}_F$ sector) and $1D$-wave states in this paper, their mass values and the root-mean-square radii are listed in Tables 4-7 of Appendix D, and the corresponding mass spectra are presented in Fig. 2.

A. Structure properties of singly heavy baryon spectra

(1) Contribution of each Hamiltonian term.

In these Hamiltonian terms, $\langle H_{mode}\rangle \equiv \langle H_0 + H^{conf}\rangle$ depends on the excitation modes (l_ρ, l_λ) and dominates the main part of the energy levels. The other terms affect the shift and splitting of the energy levels. It is clearly displayed in Table 3. As is shown in Table 3, the tensor terms have little influence on the energy levels. The contact term $\langle H^c_{12}\rangle$ causes a big shift of the energy levels, nevertheless, has little effect on the energy level splitting. For the Σ_c baryons, the contribution of the contact term $\langle H^c_{23(31)}\rangle$ to the energy level splitting decreases by orders of magnitude with the increase of L.

For the spin-orbit terms, $\langle H^{SO(v)}_{12}\rangle$ and $\langle H^{SO(s)}_{12}\rangle$ are equal to 0. The reason lies in that they are only related with l_ρ. In the (0,1) and (0,2) excitation modes ($l_\rho = 0$), $\langle H^{SO(v)}_{12}\rangle$ and $\langle H^{SO(s)}_{12}\rangle$ vanish. While in the (1,0) mode ($l_\rho = 1$) of the Σ_c baryons, they are still equal to zero due

Table 4. Calculated $\langle r^2_\rho\rangle^{1/2}$, $\langle r^2_\lambda\rangle^{1/2}$ (in fm) and mass values (in MeV) for the $1S$-, $2S$-, $3S$-, $1P$-, $2P$- and $1D$-wave states of the $\Lambda_{c(b)}$ and $\Xi_{c(b)}$ baryons. The experimental data are also listed for comparison, taken by their isospin averages.

$(l_\rho,l_\lambda)nL(J^P)_j$	$\langle r^2_\rho\rangle^{1/2}$	$\langle r^2_\lambda\rangle^{1/2}$	$M_{cal.}$	Baryon/$M_{exp.}$/$J^P_{exp.}$	$\langle r^2_\rho\rangle^{1/2}$	$\langle r^2_\lambda\rangle^{1/2}$	$M_{cal.}$	Baryon/$M_{exp.}$/$J^P_{exp.}$
			Λ_c				Λ_b	
$(0,0)1S(\frac{1}{2}^+)_0$	0.512	0.444	2288	$\Lambda_c^+/\sim 2286/\frac{1}{2}^+$ [2]	0.519	0.407	5622	$\Lambda_b^0/\sim 5620/\frac{1}{2}^+$ [2]
$(0,0)2S(\frac{1}{2}^+)_0$	0.631	0.786	2764	$\Lambda_c(2765)^+/\sim 2767/?^?$ [2]	0.599	0.716	6041	$\Lambda_b(6070)^0/\sim 6072/\frac{1}{2}^+$ [2]
$(0,0)3S(\frac{1}{2}^+)_0$	0.988	0.633	3022	–	0.953	0.677	6352	–
$(0,1)1P(\frac{1}{2}^-)_1$	0.541	0.633	2597	$\Lambda_c(2595)^+/\sim 2592/\frac{1}{2}^-$ [2]	0.536	0.579	5899	$\Lambda_b(5912)^0/\sim 5912/\frac{1}{2}^-$ [2]
$(0,1)1P(\frac{3}{2}^-)_1$	0.545	0.660	2631	$\Lambda_c(2625)^+/\sim 2628/\frac{3}{2}^-$ [2]	0.538	0.589	5913	$\Lambda_b(5920)^0/\sim 5920/\frac{3}{2}^-$ [2]
$(0,1)2P(\frac{1}{2}^-)_1$	0.607	0.963	2990	$\Lambda_c(2910)^+/\sim$**2914**$/?^?$ [2]	0.579	0.855	6239	–
$(0,1)2P(\frac{3}{2}^-)_1$	0.602	0.991	3013	$\Lambda_c(2940)^+/\sim$**2940**$/\frac{3}{2}^-$ [2]	0.577	0.861	6249	–
$(0,2)1D(\frac{3}{2}^+)_2$	0.555	0.826	2873	$\Lambda_c(2860)^+/\sim 2856/\frac{3}{2}^+$ [2]	0.543	0.748	6135	$\Lambda_b(6146)^0/\sim 6146/\frac{3}{2}^+$ [2]
$(0,2)1D(\frac{5}{2}^+)_2$	0.556	0.851	2892	$\Lambda_c(2880)^+/\sim 2882/\frac{5}{2}^+$ [2]	0.544	0.758	6146	$\Lambda_b(6152)^0/\sim 6153/\frac{5}{2}^+$ [2]
			Ξ_c				Ξ_b	
$(0,0)1S(\frac{1}{2}^+)_0$	0.512	0.437	2479	$\Xi_c^{+,0}/\sim 2469/\frac{1}{2}^+$ [2]	0.518	0.400	5806	$\Xi_b^{0,-}/\sim 5795/\frac{1}{2}^+$ [2]
$(0,0)2S(\frac{1}{2}^+)_0$	0.645	0.768	2949	$\Xi_c(2970)^{+,0}/\sim 2966/\frac{1}{2}^+$ [2]	0.607	0.705	6224	$\Xi_b(6227)^{0,-}/\sim 6227/?^?$ [2]
$(0,0)3S(\frac{1}{2}^+)_0$	0.968	0.607	3155	–	0.990	0.549	6480	–
$(0,1)1P(\frac{1}{2}^-)_1$	0.544	0.628	2789	$\Xi_c(2790)^{+,0}/\sim 2793/\frac{1}{2}^-$ [2]	0.540	0.573	6084	$\Xi_b(6087)^0/\sim 6087/\frac{3}{2}^-$ [2]
$(0,1)1P(\frac{3}{2}^-)_1$	0.549	0.654	2820	$\Xi_c(2815)^{+,0}/\sim 2818/\frac{3}{2}^-$ [2]	0.543	0.582	6097	$\Xi_b(6100)^{0,-}/\sim 6097/\frac{3}{2}^-$ [2]
$(0,1)2P(\frac{1}{2}^-)_1$	0.616	0.950	3177	–	0.587	0.846	6422	–
$(0,1)2P(\frac{3}{2}^-)_1$	0.612	0.977	3199	–	0.585	0.852	6431	–
$(0,2)1D(\frac{3}{2}^+)_2$	0.563	0.822	3061	$\Xi_c(3055)^+/\sim 3056/\frac{3}{2}^+$ [2]	0.552	0.742	6318	$\Xi_b(6327)^0/\sim 6327/?^?$ [2]
$(0,2)1D(\frac{5}{2}^+)_2$	0.564	0.845	3078	$\Xi_c(3080)^{+,0}/\sim 3079/\frac{5}{2}^+$ [2]	0.553	0.752	6328	$\Xi_b(6333)^0/\sim 6333/?^?$ [2]

Table 5. Calculated $\langle r_\rho^2\rangle^{1/2}$, $\langle r_\lambda^2\rangle^{1/2}$ (in fm) and mass values (in MeV) for the $1S$-, $2S$-, $3S$-, $1P$- and $1D$-wave states of the Σ_c and Σ_b baryons. The orbital excited states of the ρ-mode are marked in bold type. The experimental data are also listed for comparison, taken by their isospin averages.

$(l_\rho,l_\lambda)nL(J^P)_j$	$\langle r_\rho^2\rangle^{1/2}$	$\langle r_\lambda^2\rangle^{1/2}$	$M_{cal.}$	Baryon/$M_{exp.}$/$J^P_{exp.}$	$\langle r_\rho^2\rangle^{1/2}$	$\langle r_\lambda^2\rangle^{1/2}$	$M_{cal.}$	Baryon/$M_{exp.}$/$J^P_{exp.}$
			Σ_c				Σ_b	
$(0,0)1S(\frac{1}{2}^+)_1$	0.611	0.450	2456	$\Sigma_c(2455)^{++,+,0}/\sim2453/\frac{1}{2}^+$ [2]	0.631	0.433	5821	$\Sigma_b^{+,-}/\sim5813/\frac{1}{2}^+$ [2]
$(0,0)1S(\frac{3}{2}^+)_1$	0.645	0.493	2534	$\Sigma_c(2520)^{++,+,0}/\sim2518/\frac{3}{2}^+$ [2]	0.645	0.449	5849	$\Sigma_b^{*+,-}/\sim5833/\frac{3}{2}^+$ [2]
$(0,0)2S(\frac{1}{2}^+)_1$	0.841	0.732	2913	–	0.774	0.716	6226	–
$(0,0)2S(\frac{3}{2}^+)_1$	0.837	0.783	2967	–	0.770	0.734	6246	–
$(0,0)3S(\frac{1}{2}^+)_1$	0.945	0.718	3109	–	1.019	0.607	6439	–
$(0,0)3S(\frac{3}{2}^+)_1$	0.992	0.696	3127	–	1.041	0.594	6446	–
$(0,1)1P(\frac{1}{2}^-)_0$	0.658	0.640	2773	–	0.652	0.593	6087	–
$(0,1)1P(\frac{1}{2}^-)_1$	0.662	0.647	2778	$\Sigma_c(2800)^{++,+,0}/\sim2800/?^?$ [2]	0.658	0.603	6092	$\Sigma_b(6097)^{+,-}/\sim6097/?^?$ [2]
$(0,1)1P(\frac{3}{2}^-)_1$	0.670	0.672	2810	–	0.661	0.613	6105	–
$(0,1)1P(\frac{3}{2}^-)_2$	0.678	0.688	2816	–	0.673	0.636	6113	–
$(\mathbf{1},\mathbf{0})1P(\frac{1}{2}^-)_1$	0.857	0.486	2828	$\Sigma_c(2846)^0/\sim2846/?^?$ [5]	–	–	–	–
$(0,1)1P(\frac{5}{2}^-)_2$	0.689	0.731	2863	–	0.679	0.652	6133	–
$(\mathbf{1},\mathbf{0})1P(\frac{3}{2}^-)_1$	0.875	0.505	2877	–	–	–	–	–
$(0,2)1D(\frac{1}{2}^+)_1$	0.683	0.817	3048	–	0.667	0.755	6330	–
$(0,2)1D(\frac{3}{2}^+)_1$	0.684	0.834	3063	–	0.668	0.761	6337	–
$(0,2)1D(\frac{3}{2}^+)_2$	0.690	0.846	3062	–	0.675	0.778	6334	–
$(0,2)1D(\frac{5}{2}^+)_2$	0.691	0.871	3083	–	0.677	0.789	6345	–
$(0,2)1D(\frac{5}{2}^+)_3$	0.700	0.891	3076	–	0.688	0.814	6338	–
$(0,2)1D(\frac{7}{2}^+)_3$	0.702	0.923	3102	–	0.690	0.828	6351	–

to $s_{12}=0$ here, which is constrained by the condition $(-1)^{l_\rho+s_{12}}=-1$. So, the contribution of the spin-orbit terms comes only from the $\langle H_{23}^{SO}\rangle$ and the $\langle H_{31}^{SO}\rangle$. From Table 3, one can see the $\langle H_{23(31)}^{SO(v)}\rangle$ and the $\langle H_{23(31)}^{SO(s)}\rangle$ always partially cancel each other out. But, they jointly lead to the shift and splitting of the energy levels. Especially, in the (1,0) mode, they cause a big splitting of the energy levels, which makes the $(\mathbf{1},\mathbf{0})1P(\frac{1}{2}^-)_1$ state intrude into the region of the $(0,1)1P$ states.

For the energy level splitting, the contribution of the spin-orbit terms is bigger than that of the contact terms. So, the spin-orbit interaction is very important for the excitation spectra structure of the singly heavy baryons.

(2) Heavy-quark dominance.

The HQD mechanism and its breaking in the orbital excitation of the heavy baryons were proposed and investigated in Refs. [49, 50], and the HQD mechanism dominates the structure of the excitation spectra. This mechanism means that the excitation mode with lower energy levels is always associated with the heavy quark(s), and the splitting of the energy levels is suppressed by the heavy quark(s) as well. In other words, the heavy quarks dominate the orbital excitation of singly and doubly heavy baryons, and determine the structures of their excitation spectra. The HQD mechanism is generally effective. But for the $1P$-wave orbital excitation of the singly charm baryons, it is slightly broken, since c quark is not heavy enough. From Tables 4-7, the results show that the mechanism holds up well under the rigorous calculation.

(3) Fine structures.

As is shown in Tables 5-7 and Fig. 2, the rigorous

Table 6. Same as Table V, but for the Ξ_c' and Ξ_b' baryons.

$(l_\rho,l_\lambda)nL(J^P)_j$	$\langle r_\rho^2\rangle^{1/2}$	$\langle r_\lambda^2\rangle^{1/2}$	$M_{cal.}$	Baryon/$M_{exp.}$/$J^P_{exp.}$	$\langle r_\rho^2\rangle^{1/2}$	$\langle r_\lambda^2\rangle^{1/2}$	$M_{cal.}$	Baryon/$M_{exp.}$/$J^P_{exp.}$
			Ξ_c'				Ξ_b'	
$(0,0)1S(\frac{1}{2}^+)_1$	0.584	0.435	2589	$\Xi_c'^{+,0}$/~2578/$\frac{1}{2}^+$ [2]	0.602	0.414	5944	$\Xi_b'(5935)^-$/~5935/$\frac{1}{2}^+$ [2]
$(0,0)1S(\frac{3}{2}^+)_1$	0.614	0.474	2660	$\Xi_c(2645)^{+,0}$/~2645/$\frac{3}{2}^+$ [2]	0.615	0.430	5971	$\Xi_b(5955)^{0,-}$/~5954/$\frac{3}{2}^+$ [2]
$(0,0)2S(\frac{1}{2}^+)_1$	0.809	0.714	3046	–	0.739	0.699	6351	–
$(0,0)2S(\frac{3}{2}^+)_1$	0.804	0.762	3096	–	0.735	0.715	6369	–
$(0,0)3S(\frac{1}{2}^+)_1$	0.925	0.685	3220	–	0.999	0.570	6543	–
$(0,0)3S(\frac{3}{2}^+)_1$	0.967	0.668	3237	–	1.017	0.561	6551	–
$(0,1)1P(\frac{1}{2}^-)_0$	0.633	0.628	2906	$\Xi_c(2882)^0$/~2882/? [2]	0.629	0.578	6214	–
$(0,1)1P(\frac{1}{2}^-)_1$	0.636	0.634	2912	–	0.633	0.587	6218	–
$(0,1)1P(\frac{3}{2}^-)_1$	0.644	0.658	2941	$\Xi_c(2923)^{+,0}$/~2923/? [2, 22]	0.636	0.596	6230	–
$(0,1)1P(\frac{3}{2}^-)_2$	0.649	0.670	2948	$\Xi_c(2930)^{+,0}$/~2941/? [2]	0.645	0.614	6237	–
$(\mathbf{1},\mathbf{0})1P(\frac{1}{2}^-)_1$	0.828	0.473	2958	–	–	–	–	–
$(0,1)1P(\frac{5}{2}^-)_2$	0.660	0.709	2990	–	0.650	0.629	6256	–
$(\mathbf{1},\mathbf{0})1P(\frac{3}{2}^-)_1$	0.847	0.490	3004	–	–	–	–	–
$(0,2)1D(\frac{1}{2}^+)_1$	0.660	0.808	3177	$\Xi_c(3123)^+$/~3123/? [2]	0.647	0.742	6452	–
$(0,2)1D(\frac{3}{2}^+)_1$	0.662	0.824	3189	–	0.647	0.748	6458	–
$(0,2)1D(\frac{3}{2}^+)_2$	0.666	0.833	3190	–	0.653	0.761	6456	–
$(0,2)1D(\frac{5}{2}^+)_2$	0.668	0.856	3208	–	0.655	0.771	6466	–
$(0,2)1D(\frac{5}{2}^+)_3$	0.674	0.870	3207	–	0.663	0.790	6461	–
$(0,2)1D(\frac{7}{2}^+)_3$	0.676	0.899	3229	–	0.665	0.804	6473	–

calculation reveals the perfect fine structures of the excitation spectra, not only for all the $1P$-wave states, but also for the $1D$-wave states of the charm baryons Σ_c, Ξ_c' and Ω_c. According to the data of the Ω_c baryons, the fine structure of the $1P$-excited charm baryons (Σ_c, Ξ_c' and Ω_c) should be composed of the 5 energy levels which are the $(0,1)1P(\frac{1}{2}^-)_{0,1}$, $(0,1)1P(\frac{3}{2}^-)_{1,2}$, $(1,0)1P(\frac{1}{2}^-)_1$ (as an intrude state), $(0,1)1P(\frac{5}{2}^-)_2$ and $(1,0)1P(\frac{3}{2}^-)_1$, respectively. Based on the data of the Ω_b baryons, however, the fine structure of the $1P$-wave states of the bottom baryons (Σ_b, Ξ_b' and Ω_b) may contain the 4 energy levels, they are the $(0,1)1P(\frac{1}{2}^-)_{0,1}$, $(0,1)1P(\frac{3}{2}^-)_1$, $(0,1)1P(\frac{3}{2}^-)_2$ and $(0,1)1P(\frac{5}{2}^-)_2$, respectively. For the $1D$-wave states of the Σ_c, Ξ_c' and Ω_c baryons, there are clear and distinct 4 energy levels as shown in Fig. 2. The predicted fine structure of the $1D$-wave states has yet to be confirmed by the future experiments.

(4) Missing states.

In the relativized quark model, the calculations in Refs. [27, 28] predicted a substantial number of 'missing' states, compared to the experimental observations of the singly heavy baryons. The practice of reducing the internal degrees of freedom, such as the heavy quark-light diquark picture [34], predicted significantly fewer states than the former, however, lacks a reasonable physical explanation [1, 56]. Now, under the HQD mechanism, the rigorous calculation can reproduce well the data, and the problem of the missing states disappears thereof. So, the HQD mechanism in the genuine three-body picture might be a natural solution to the missing states.

(5) Clustering effect.

The heavy quark-light diquark picture achieved great successes in describing the spectra of the singly heavy baryons, based on an important concept of the 'diquark' or the quark cluster [34]. By taking account of the contribution of the quark cluster, the fine structure was prelimin-

Table 7. Same as Table 5, but for the Ω_c and Ω_b baryons.

$(l_\rho,l_\lambda)nL(J^P)_j$	$\langle r_\rho^2\rangle^{1/2}$	$\langle r_\lambda^2\rangle^{1/2}$	$M_{cal.}$	Baryon/$M_{exp.}$/$J^P_{exp.}$	$\langle r_\rho^2\rangle^{1/2}$	$\langle r_\lambda^2\rangle^{1/2}$	$M_{cal.}$	Baryon/$M_{exp.}$/$J^P_{exp.}$
			Ω_c				Ω_b	
$(0,0)1S(\frac{1}{2}^+)_1$	0.549	0.417	2696	Ω_c^0/~2695/$\frac{1}{2}^+$ [2]	0.564	0.395	6043	Ω_b^-/~6045/$\frac{1}{2}^+$ [2]
$(0,0)1S(\frac{3}{2}^+)_1$	0.578	0.454	2765	$\Omega_c(2770)^0$/~2766/$\frac{3}{2}^+$ [2]	0.576	0.409	6069	–
$(0,0)2S(\frac{1}{2}^+)_1$	0.775	0.686	3150	–	0.705	0.672	6448	–
$(0,0)2S(\frac{3}{2}^+)_1$	0.771	0.730	3198	$\Omega_c(3185)^0$/~3185/?[?] [2]	0.702	0.687	6465	–
$(0,0)3S(\frac{1}{2}^+)_1$	0.882	0.672	3325	$\Omega_c(3327)^0$/~3327/?[?] [2]	0.953	0.560	6641	–
$(0,0)3S(\frac{3}{2}^+)_1$	0.924	0.654	3339	–	0.973	0.549	6647	–
$(0,1)1P(\frac{1}{2}^-)_0$	0.602	0.605	3009	$\Omega_c(3000)^0$/~3000/?[?] [2]	0.595	0.552	6308	$\Omega_b(6316)^-$/~6315/?[?] [2]
$(0,1)1P(\frac{1}{2}^-)_1$	0.604	0.609	3015	–	0.599	0.560	6313	–
$(0,1)1P(\frac{3}{2}^-)_1$	0.612	0.633	3045	$\Omega_c(3050)^0$/~3050/?[?] [2]	0.602	0.570	6326	$\Omega_b(6330)^-$/~6330/?[?] [2]
$(0,1)1P(\frac{3}{2}^-)_2$	0.615	0.643	3052	–	0.608	0.586	6334	$\Omega_b(6340)^-$/~6340/?[?] [2]
$(\mathbf{1},\mathbf{0})1P(\frac{1}{2}^-)_1$	0.792	0.459	3059	$\Omega_c(3065)^0$/~3065/?[?] [2]	–	–	–	–
$(0,1)1P(\frac{5}{2}^-)_2$	0.626	0.683	3095	$\Omega_c(3090)^0$/~3090/?[?] [2]	0.614	0.601	6353	$\Omega_b(6350)^-$/~6350/?[?] [2]
$(\mathbf{1},\mathbf{0})1P(\frac{3}{2}^-)_1$	0.813	0.479	3109	$\Omega_c(3120)^0$/~3119/?[?] [2]	–	–	–	–
$(0,2)1D(\frac{1}{2}^+)_1$	0.631	0.782	3278	–	0.616	0.713	6544	–
$(0,2)1D(\frac{3}{2}^+)_1$	0.633	0.801	3292	–	0.617	0.720	6552	–
$(0,2)1D(\frac{3}{2}^+)_2$	0.635	0.806	3293	–	0.621	0.731	6550	–
$(0,2)1D(\frac{5}{2}^+)_2$	0.637	0.831	3311	–	0.622	0.742	6561	–
$(0,2)1D(\frac{5}{2}^+)_3$	0.640	0.840	3310	–	0.627	0.759	6557	–
$(0,2)1D(\frac{7}{2}^+)_3$	0.642	0.871	3332	–	0.629	0.772	6570	–

arily explained in our previous work [50], which hints that there might be the clustering effect inside a singly heavy baryon. Now, the rigorous calculation shows that, without introducing the concept of the 'diquark' or the quark cluster, the excitation spectra and their fine structures can also be reproduced very well. So, there is no indication that the clustering effect is indispensable inside a singly heavy baryon.

(6) Spin-orbit terms.

In both the light-quark baryons and the heavy-quark baryons, the treatment of the spin-orbit terms used to be a difficult problem [29, 51, 52]. This is mainly due to the following two reasons. One is that the experimental data were not sufficient, and the other is that the rigorous model calculation was difficult. Both difficulties have now been overcome in the research of the singly heavy baryons, i.e., there are enough experimental data currently and the rigorous calculations has been implemented. Table3 shows clearly the contribution of each spin-orbit term, which demonstrates its irreplaceable role in accurately reproducing the fine structures. And an earlier assertion is confirmed here, namely, the contribution of the spin-orbit terms must indeed be fully considered before the fine structures can be well explained in the singly heavy baryon spectra [29]. Therefore, based on this study, it is concluded that the spin-orbit terms of the relativized quark model are reasonable for describing the singly heavy baryon spectra, and the 'spin-orbit puzzle' [29, 51, 52] does not exist anymore here. Note that this work ignores the mixing between different excited states, whose effect on the energy levels still needs to be further studied.

B. Excitation spectra and experimental data

In our previous works, the assignments of the observed baryons have been discussed, and a detailed com-

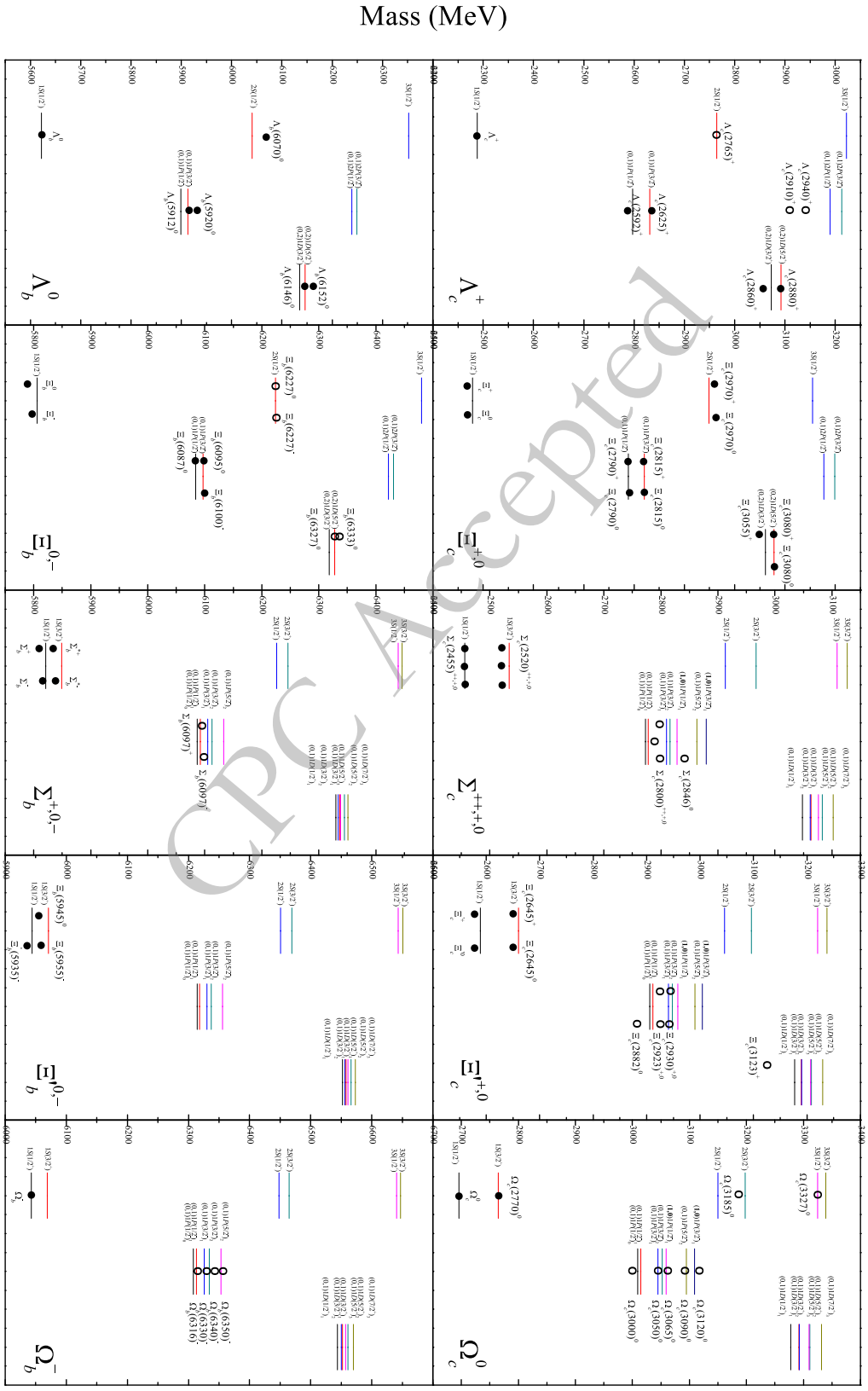

Fig. 2. Calculated spectra of the singly heavy baryons and the relevant experimental data [2, 5, 22]. '++','+', '0' and '-' in the brackets indicate the charged states of baryons. The solid black circles denote the baryons with confirmed spin-parity values, and the open circles are the ones whose spin-parities have not been identified.

parison of our results with other theoretical estimations has been presented as well [44, 45, 49, 50]. In this work, the rigorous calculation mainly improves the results of the fine structure. So, the following discussion will focus on the systematic analysis of the model calculations, by comparing the predicted excitation spectra with the experimental data.

All of the observed masses of the singly heavy baryons and the predicted spectra are plotted together in Fig. 2. The detailed experimental data and calculated results are listed in Tables 4-7, for the $\Lambda_{c(b)}$, $\Xi_{c(b)}$, $\Sigma_{c(b)}$, $\Xi'_{c(b)}$ and $\Omega_{c(b)}$ baryons, respectively. As is shown in Fig. 2 and Tables 4-7, most of the observed masses match well with the predicted spectra, and the maximum deviation between the calculated masses and the data is generally not more than 20 MeV.

(1) $\Lambda_{c(b)}$ and $\Xi_{c(b)}$ baryons.

The $\Lambda_{c(b)}$ and $\Xi_{c(b)}$ baryons belong to the $\bar{\mathbf{3}}_F$ sector. They have the same spectral structure. Fig. 2 shows that the match between the calculation results and the data is good on the whole, except for the $\Lambda_c(2910)^+$ and the $\Lambda_c(2940)^+$. The $\Lambda_c(2940)^+$ was measured by the LHCb collaboration in 2017 [6], and a narrow peak was seen in pD^0 and in $\Lambda_c^+\pi^+\pi^-$. It was not seen in pD^+, and therefore it might be a Λ_c^+ baryon. Its $J^P = 3/2^-$ is favored, but not certain [2]. The $\Lambda_c(2910)^+$ was reported by the Belle collaboration in 2022 [17]. It was considered as the candidate of the heavy quark symmetry doublet partner to the $\Lambda_c(2940)^+$ [2]. In Fig. 2, one can see these two baryons have to be assigned as the $2P$-doublet states, if they belong to the Λ_c family. However, the difference between their measured masses and predicted ones is so big that it is far beyond the allowable error range of the theoretical calculation. So, the $\Lambda_c(2910)^+$ and $\Lambda_c(2940)^+$ are probably not the members of the Λ_c family. In some theoretical studies, they were considered as the molecular states [35, 57]. If only their mass values are considered, however, they are more like the candidates of the $2S$-doublet states in the Σ_c family as shown in Fig. 2 and Table 5. It needs to be further confirmed by experiments.

The $\Xi_b(6227)^{0,-}$ baryons were measured precisely by the LHCb collaboration in 2021 [15], but their J^P values remain unconfirmed. According to their mass values, the $\Xi_b(6227)^{0,-}$ baryons could be assigned as the $2S(\frac{1}{2}^+)$ state of the Ξ_b family as shown in Fig. 2. Alternatively, they might be the candidates of the $1P(\frac{1}{2}^-)_{0,1}$ state or the $1P(\frac{3}{2}^-)_1$ state of the Ξ'_b family.

(2) Σ_c and Σ_b baryons.

The $\Sigma_c(2800)^{++,+,0}$ baryons were reported by the Belle Collaboration in 2005 [3]. The $\Sigma_c(2846)^0$ was observed by the BaBar collaboration, with $m = 2846 \pm 8 \pm 10$ MeV [5], which has not been collected by the PDG so far. In this work, it is assumed to be a real baryon. Based on the calculation, the $\Sigma_c(2846)^0$ and the $\Sigma_c(2800)^{++,+,0}$ are in the region of the $1P$-wave states. By examining their mass values and the fine structure of the $1P$-wave states shown in Fig. 2, the $\Sigma_c(2800)^{++,+,0}$ could be assigned as the $(0,1)1P(\frac{1}{2}^-)_{0,1}$ states, and the $\Sigma_c(2846)^0$ could be considered as the intrude state $(1,0)1P(\frac{1}{2}^-)_1$.

The case of the $\Sigma_b(6097)^{+,-}$ is similar to that of the $\Sigma_c(2800)^{++,+,0}$. So, we can safely conclude that the J^P of the $\Sigma_b(6097)^{+,-}$ is likely to be $\frac{1}{2}^-$. And they should be the $(0,1)1P(\frac{1}{2}^-)_{0,1}$ states.

(3) Ξ'_c and Ξ'_b baryons.

A charged $\Xi_c(2930)^+$ baryon was observed by the Belle collaboration in 2018 [11]. Later, the $\Xi_c(2923)^0$, $\Xi_c(2939)^0$ and $\Xi_c(2964)^0$ states were observed with a large significance by the LHCb collaboration [14]. Very recently, a new charmed baryon $\Xi_c(2923)^+$ was firstly observed by the LHCb collaboration [22]. In the new PDG data, these baryons were relabeled as the $\Xi_c(2923)^0$, $\Xi_c(2930)^{+,0}$ and $\Xi_c(2970)^0$. The $\Xi_c(2970)^0$ and its isospin partner $\Xi_c(2970)^+$ are assigned as the $2S(\frac{1}{2}^+)$ state of the Ξ_c family [2]. While the $\Xi_c(2882)^0$ [18], $\Xi_c(2923)^{+,0}$ and $\Xi_c(2930)^{+,0}$ exhibit the fine structure of the $1P$-wave states in the Ξ'_c family. As is shown in Fig. 2, their assignments could be the $(0,1)1P(\frac{1}{2}^-)_{0,1}$, $(0,1)1P(\frac{3}{2}^-)_{1,2}$ and $(1,0)1P(\frac{1}{2}^-)_1$ states, respectively.

The $\Xi_c(3123)^+$ was observed by the BaBar Collaboration in 2007 [4]. It is difficult to make a good assignment for the $\Xi_c(3123)^+$. As is shown in Fig. 2, we consider it as a candidate of the $1D$-wave state, even though its mass value is too small. Alternatively, it could be the $2S(\frac{3}{2}^+)$ state.

If we assume that the $\Xi_b(6227)^{0,-}$ baryons are the strange partner of the $\Sigma_b(6097)^{+,-}$, we find there are great similarities between them. So, the $\Xi_b(6227)^{0,-}$ baryons could also be assigned as the same states as the $\Sigma_b(6097)^{+,-}$, instead of the $2S(\frac{1}{2}^+)$ state of the Ξ_b family as mentioned above.

(4) Ω_c and Ω_b baryons.

For these two families, the predicted fine structures of the $1P$-wave states reproduce the data perfectly, as shown in Fig. 2. Their assignments are listed in Table 7. The $\Omega_c(3185)^0$ is likely to be the $2S(\frac{3}{2}^+)$ state. The $\Omega_c(3327)^0$ is assigned as the $3S(\frac{1}{2}^+)$ state, but its mass value overlaps with those of the $1D$-wave states.

(5) Baryons in the fine structures.

The $\Sigma_c(2800)^{++,+,0}$, $\Sigma_c(2846)^0$ and $\Sigma_b(6097)^{+,-}$ have a common feature, i.e., their decay widths are much more than 15 MeV. For the Ξ'_c, Ω_c and Ω_b baryons in the fine structures, however, their decay widths are overall smaller than 15 MeV. Given the similarity in the spectral structure of these $\Sigma_{c(b)}$, $\Xi'_{c(b)}$ and $\Omega_{c(b)}$ families, it may be true that the decay widths of the baryons in the fine structures could all be small. From this point of view, the $\Sigma_c(2800)^{++,+,0}$, $\Sigma_c(2846)^0$ and $\Sigma_b(6097)^{+,-}$ might be the su-

perpositions of several quantum states, and that more precise measurements may reveal their fine structures further. The $\Xi_b(6227)^{0,-}$ would have the same problem if they belong to the Ξ_b' family, as well as the assignment of the $\Omega_c(3327)^0$ as mentioned above.

In Ref. [58], the following chain was found by analyzing the universal behavior of the mass gaps of the baryons,

$$\Sigma_c(2846)^0 \leftrightarrow \Xi_c'(2964)^0 \leftrightarrow \Omega_c(3090)^0, \tag{15}$$

which implies that these baryons are in the same quantum state. Now, the $\Xi_c(2964)^0$ (relabeled as $\Xi_c(2970)^0$) has been considered as the member of the Ξ_c family. As is shown in Fig. 2, the updated chain should be as follow,

$$\Sigma_c(2846)^0 \leftrightarrow \Xi_c'(2930)^0 \leftrightarrow \Omega_c(3065)^0, \tag{16}$$

if the $\Sigma_c(2846)^0$ is a single state.

C. Reliability of the model

Some approximate calculations were adopted in our previous works actually. In Refs. [44, 45], the $\tilde{H}_{13}^{hyp}$ and $\tilde{H}_{23}^{hyp}$ terms were ignored in the hyperfine interaction. The spin-orbit interaction only contained the $\tilde{H}_{12}^{SO}$ term coming from the light quark pair and a part of the $\tilde{H}_{d-Q}^{SO}$ term contributed jointly by the heavy quark (Q) and the light-diquark (d) (only including the leading order contribution as the Eq.(33) in Ref. [52]). In Ref. [50], the light-diquark approximation was considered completely, where the hyperfine interaction was represented by the $\tilde{H}_{12}^{hyp}$ and $\tilde{H}_{d-Q}^{hyp}$ terms, and the spin-orbit interaction contained the $\tilde{H}_{12}^{SO}$ and $\tilde{H}_{d-Q}^{SO}$ terms. In this work, all of the Hamiltonian terms are obtained without approximation. As a result, most of the energy levels of the excited states in this work are shifted, even for some of the S-wave radial excited states, compared to those in our previous works.

Since the parameters used in the present work are given without any uncertainty, they certainly do not result in any uncertainty in the calculated results. We here evaluate the deviations of the calculated masses of the 74 baryons from the measured ones as shown in Table 8. Most of the deviations are less than 20 MeV. And the arithmetic average deviation is less than 10 MeV, which is consistent with the estimation result in Ref. [26].

As is shown in Fig. 2 and Table 8, the predicted mass spectra in this work can reproduce the data nicely on the whole, for all the singly heavy baryon families. The shell structure of the spectra is clearly shown. It implies that this model can successfully describe the singly heavy baryon spectra without approximation.

The fine structures can be reproduced well, especially for the Ω_c and Ω_b families. It shows the rationality of the Hamiltonian based on the two-body interactions of the relativized quark model.

While, for the excitation spectrum of each family, there is a little systematic deviation between the predicted mass values and the data. For a few baryons, such as the $\Xi_c(3123)^+$, the theoretical results cannot explain the data reasonably. So, some improvements of this model should be tried, such as a parameter optimization.

In summary, under the HQD mechanism, the relativized quark model can describe the excitation spectra and the fine structures correctly. Based on the relativized quark model, the method used in this work should be reliable in the research of the singly heavy baryons spectroscopy.

IV. CONCLUSIONS

In this work, the rigorous calculation of the spin-orbit terms of the relativized quark model is realized based on the GEM and the ISG basis functions, by ignoring the mixing between different excited states. Then, the complete mass spectra of the singly heavy baryons are obtained rigorously in the framework of the relativized quark model and under the HQD mechanism. On these bases, the systematical analyses are carried out for the reliability and predictive power of the model, the fine structure of the singly heavy baryon spectra, the assignments of the excited baryons, and some important topics about the heavy baryon spectroscopy, such as the missing states, the clustering effect, the 'spin-orbit puzzle', etc.

The main work done and main results obtained in the present paper are as follows:

(1) The contribution of each Hamiltonian term to the energy levels is figured out.

(2) The HQD mechanism is further confirmed.

(3) The fine structures of the singly heavy baryons are presented.

(4) The missing states in the singly heavy baryon spectra disappear naturally under the HQD mechanism.

(5) There is no indication that the clustering effect is indispensable in a singly heavy baryon.

(6) The spin-orbit terms of the relativized quark model are reasonable for describing the singly heavy baryon spectra, and the 'spin-orbit puzzle' does not exist here.

(7) The $\Lambda_c(2910)^+$ and $\Lambda_c(2940)^+$ are probably not the members of the Λ_c family. While, they are more like the candidates of the $2S$-doublet states in the Σ_c family, if only their mass values are considered.

(8) It is difficult to make a good assignment for the $\Xi_c(3123)^+$ in this work.

(9) The $\Sigma_c(2800)^{++,+,0}$, $\Sigma_c(2846)^0$ and $\Sigma_b(6097)^{+,-}$ may not be single states, and more precise measurements are advised for uncovering their fine structures further.

In summary, the rigorous calculation shows that under the HQD mechanism, the relativized quark model can

Table 8. The deviations of the calculated masses of the 74 baryons from the measured ones [2, 5, 22]. Most of the deviations are less than 20 MeV. The arithmetic average deviation $(\sum_{i=1}^{n}|M_{cal.}-M_{exp.}|_i)/n$ is about 9.12 MeV. $M_{exp.}$ denotes the central value of the measured mass. '↑' means the same as above. The $\Lambda_c(2910)^+$, $\Lambda_c(2940)^+$ and $\Xi_c(3123)^+$ are not included in the list.

Baryon (J^P)	$M_{exp.}$	$(l_\rho,l_\lambda)nL(J^P)_j$	$M_{cal.}$	$M_{cal.}-M_{exp.}$	Baryon (J^P)	$M_{exp.}$	$(l_\rho,l_\lambda)nL(J^P)_j$	$M_{cal.}$	$M_{cal.}-M_{exp.}$
$\Lambda_c^+(\frac{1}{2}^+)$	2286.46	$(0,0)1S(\frac{1}{2}^+)_0$	2288	1.54	$\Omega_c(2770)^0(\frac{3}{2}^+)$	2766	$(0,0)1S(\frac{3}{2}^+)_1$	2765	−1
$\Lambda_c(2595)^+(\frac{1}{2}^-)$	2592.25	$(0,1)1P(\frac{1}{2}^-)_1$	2597	4.75	$\Omega_c(3000)^0(?^?)$	3000.46	$(0,1)1P(\frac{1}{2}^-)_0$	3009	8.54
$\Lambda_c(2625)^+(\frac{3}{2}^-)$	2628	$(0,1)1P(\frac{3}{2}^-)_1$	2631	3	$\Omega_c(3050)^0(?^?)$	3050.17	$(0,1)1P(\frac{3}{2}^-)_1$	3045	−5.17
$\Lambda_c(2765)^+(?^?)$	2766.6	$(0,0)2S(\frac{1}{2}^+)_0$	2764	−2.6	$\Omega_c(3065)^0(?^?)$	3065.58	$(1,0)1P(\frac{1}{2}^-)_1$	3059	−6.58
$\Lambda_c(2860)^+(\frac{3}{2}^+)$	2856.1	$(0,2)1D(\frac{3}{2}^+)_2$	2873	16.9	$\Omega_c(3090)^0(?^?)$	3090.15	$(0,1)1P(\frac{5}{2}^-)_2$	3095	4.85
$\Lambda_c(2880)^+(\frac{5}{2}^+)$	2881.62	$(0,2)1D(\frac{5}{2}^+)_2$	2892	10.38	$\Omega_c(3120)^0(?^?)$	3118.98	$(1,0)1P(\frac{3}{2}^-)_1$	3109	−9.98
$\Sigma_c(2455)^{++}(\frac{1}{2}^+)$	2453.97	$(0,0)1S(\frac{1}{2}^+)_1$	2456	2.03	$\Omega_c(3185)^0(?^?)$	3185	$(0,0)2S(\frac{3}{2}^+)_1$	3198	13
$\Sigma_c(2455)^+(\frac{1}{2}^+)$	2452.65	↑	↑	3.35	$\Omega_c(3327)^0(?^?)$	3327.1	$(0,0)3S(\frac{1}{2}^+)_1$	3325	−2.1
$\Sigma_c(2455)^0(\frac{1}{2}^+)$	2453.75	↑	↑	2.25	$\Lambda_b^0(\frac{1}{2}^+)$	5619.5	$(0,0)1S(\frac{1}{2}^+)_0$	5622	2.43
$\Sigma_c(2520)^{++}(\frac{3}{2}^+)$	2518.42	$(0,0)1S(\frac{3}{2}^+)_1$	2534	15.59	$\Lambda_b(5912)^0(\frac{1}{2}^-)$	5912.16	$(0,1)1P(\frac{1}{2}^-)_1$	5899	−13.2
$\Sigma_c(2520)^+(\frac{3}{2}^+)$	2517.4	↑	↑	16.6	$\Lambda_b(5920)^0(\frac{3}{2}^-)$	5920.07	$(0,1)1P(\frac{3}{2}^-)_1$	5913	−7.07
$\Sigma_c(2520)^0(\frac{3}{2}^+)$	2518.48	↑	↑	15.52	$\Lambda_b(6070)^0(\frac{1}{2}^+)$	6072.3	$(0,0)2S(\frac{1}{2}^+)_0$	6041	−31.3
$\Sigma_c(2800)^{++}(?^?)$	2801	$(0,1)1P(\frac{1}{2}^-)_1$	2778	−23	$\Lambda_b(6146)^0(\frac{3}{2}^+)$	6146.2	$(0,2)1D(\frac{3}{2}^+)_2$	6135	−11.2
$\Sigma_c(2800)^+(?^?)$	2792	↑	↑	−14	$\Lambda_b(6152)^0(\frac{5}{2}^+)$	6152.5	$(0,2)1D(\frac{5}{2}^+)_2$	6146	−6.5
$\Sigma_c(2800)^0(?^?)$	2806	↑	↑	−28	$\Sigma_b^+(\frac{1}{2}^+)$	5810.56	$(0,0)1S(\frac{1}{2}^+)_1$	5821	10.44
$\Sigma_c(2846)^0(?^?)$	2846	$(1,0)1P(\frac{1}{2}^-)_1$	2828	−18	$\Sigma_b^-(\frac{1}{2}^+)$	5815.64	↑	↑	5.36
$\Xi_c^+(\frac{1}{2}^+)$	2467.95	$(0,0)1S(\frac{1}{2}^+)_0(\bar{\mathbf{3}}_F)$	2479	11.05	$\Sigma_b^{*+}(\frac{3}{2}^+)$	5830.32	$(0,0)1S(\frac{3}{2}^+)_1$	5849	18.68
$\Xi_c^0(\frac{1}{2}^+)$	2470.44	↑	↑	8.56	$\Sigma_b^{*-}(\frac{3}{2}^+)$	5834.74	↑	↑	14.26
$\Xi_c^{'+}(\frac{1}{2}^+)$	2578.2	$(0,0)1S(\frac{1}{2}^+)_1(\mathbf{6}_F)$	2589	10.8	$\Sigma_b(6097)^+(?^?)$	6095.8	$(0,1)1P(\frac{1}{2}^-)_1$	6092	−3.8
$\Xi_c^{'0}(\frac{1}{2}^+)$	2578.7	↑	↑	10.3	$\Sigma_b(6097)^-(?^?)$	6098.0	↑	↑	−6.0
$\Xi_c(2645)^+(\frac{3}{2}^+)$	2645.1	$(0,0)1S(\frac{3}{2}^+)_1(\mathbf{6}_F)$	2660	14.9	$\Xi_b^-(\frac{1}{2}^+)$	5797	$(0,0)1S(\frac{1}{2}^+)_0(\mathbf{6}_F)$	5806	9
$\Xi_c(2645)^0(\frac{3}{2}^+)$	2645.7	↑	↑	14.3	$\Xi_b^0(\frac{1}{2}^+)$	5791.7	↑	↑	14.3
$\Xi_c(2790)^+(\frac{1}{2}^-)$	2791.9	$(0,1)1P(\frac{1}{2}^-)_1(\bar{\mathbf{3}}_F)$	2789	−2.9	$\Xi_b(5935)^-(\frac{1}{2}^+)$	5934.9	$(0,0)1S(\frac{1}{2}^+)_1(\mathbf{6}_F)$	5944	9.1
$\Xi_c(2790)^0(\frac{1}{2}^-)$	2793.9	↑	↑	−4.9	$\Xi_b(5945)^0(\frac{3}{2}^+)$	5952.3	$(0,0)1S(\frac{3}{2}^+)_1(\mathbf{6}_F)$	5971	18.7
$\Xi_c(2815)^+(\frac{3}{2}^-)$	2816.51	$(0,1)1P(\frac{3}{2}^-)_1(\bar{\mathbf{3}}_F)$	2820	3.49	$\Xi_b(5955)^-(\frac{3}{2}^+)$	5955.5	↑	↑	15.5
$\Xi_c(2815)^0(\frac{3}{2}^-)$	2819.79	↑	↑	0.21	$\Xi_b(6087)^-(\frac{3}{2}^-)$	6087	$(0,1)1P(\frac{1}{2}^-)_1(\bar{\mathbf{3}}_F)$	6084	−3
$\Xi_c(2882)^0(?^?)$	2882	$(0,1)1P(\frac{1}{2}^-)_0(\mathbf{6}_F)$	2906	24	$\Xi_b(6095)^0(\frac{3}{2}^-)$	6095.1	$(0,1)1P(\frac{3}{2}^-)_1(\bar{\mathbf{3}}_F)$	6097	1.9
$\Xi_c(2923)^+(?^?)$	2922.8	$(0,1)1P(\frac{3}{2}^-)_1(\mathbf{6}_F)$	2941	18.2	$\Xi_b(6100)^-(\frac{3}{2}^-)$	6099.8	↑	↑	−2.8
$\Xi_c(2923)^0(?^?)$	2923.2	↑	↑	17.8	$\Xi_b(6227)^-(?^?)$	6227.9	$(0,0)2S(\frac{1}{2}^+)_0(\bar{\mathbf{3}}_F)$	6224	−3.9
$\Xi_c(2930)^+(?^?)$	2942	$(0,1)1P(\frac{3}{2}^-)_2(\mathbf{6}_F)$	2948	6	$\Xi_b(6227)^0(?^?)$	6226.8	↑	↑	−2.8
$\Xi_c(2930)^0(?^?)$	2938.55	↑	↑	9.45	$\Xi_b(6327)^0(?^?)$	6327.28	$(0,2)1D(\frac{3}{2}^-)_2(\bar{\mathbf{3}}_F)$	6318	−9.28
$\Xi_c(2970)^+(\frac{1}{2}^+)$	2964.3	$(0,0)2S(\frac{1}{2}^+)_0(\bar{\mathbf{3}}_F)$	2949	−15.3	$\Xi_b(6333)^0(?^?)$	6332.69	$(0,2)1D(\frac{5}{2}^-)_2(\bar{\mathbf{3}}_F)$	6328	−4.69
$\Xi_c(2970)^0(\frac{1}{2}^+)$	2965.9	↑	↑	−16.9	$\Omega_b^-(\frac{1}{2}^+)$	6045.8	$(0,0)1S(\frac{1}{2}^+)_1$	6043	−2.8
$\Xi_c(3055)^+(\frac{3}{2}^+)$	3055.9	$(0,2)1D(\frac{3}{2}^+)_2(\bar{\mathbf{3}}_F)$	3061	5.1	$\Omega_b(6316)^-(?^?)$	6315.6	$(0,1)1P(\frac{1}{2}^-)_0$	6308	−7.6
$\Xi_c(3080)^+(\frac{5}{2}^+)$	3077.2	$(0,2)1D(\frac{5}{2}^+)_2(\bar{\mathbf{3}}_F)$	3078	0.8	$\Omega_b(6330)^-(?^?)$	6330.3	$(0,1)1P(\frac{3}{2}^-)_1$	6326	−4.3
$\Xi_c(3080)^0(\frac{5}{2}^+)$	3079.9	↑	↑	−1.9	$\Omega_b(6340)^-(?^?)$	6339.7	$(0,1)1P(\frac{3}{2}^-)_2$	6334	−5.7
$\Omega_c^0(\frac{1}{2}^+)$	2695.3	$(0,0)1S(\frac{1}{2}^+)_1$	2696	0.7	$\Omega_b(6350)^-(?^?)$	6349.8	$(0,1)1P(\frac{5}{2}^-)_2$	6353	3.2

describe the excitation spectra and the fine structures of the singly heavy baryons correctly and precisely. Based on the relativized quark model, the method used in this work should be reliable in the research of the singly heavy baryons spectroscopy. And some improvements of this method should be tried later, for a deep understand-

ing of the properties of the singly heavy baryon spectroscopy and the strong interaction in the non-perturbative regime of QCD.

ACKNOWLEDGEMENTS

We thank the reviewers for their valuable comments and suggestions. JG would like to thank Professor Yinsheng Ling from Soochow University for his helpful discussion and great encouragement.

APPENDIX

A. Gaussian expansion method (GEM)

Given a set of the orbital quantum numbers $\{l, m\}$, the Gaussian basis function $|(nlm)^G\rangle$ is commonly written in position space as

$$\begin{aligned}\phi^G_{nlm}(\mathbf{r}) &= \phi^G_{nl}(r)Y_{lm}(\hat{\mathbf{r}}),\\ \phi^G_{nl}(r) &= N_{nl}r^l e^{-\nu_n r^2},\\ N_{nl} &= \sqrt{\frac{2^{l+2}(2\nu_n)^{l+3/2}}{\sqrt{\pi}(2l+1)!!}},\end{aligned} \tag{A1}$$

with

$$\nu_n = \frac{1}{r_n^2}, r_n = r_1 a^{n-1} \quad (n = 1, 2, ..., n_{max}). \tag{A2}$$

$\{r_1, a, n_{max}\}$ (or equivalently $\{n_{max}, r_1, r_{n_{max}}\}$) are the Gaussian size parameters and commonly related to the scale in question [54]. The optimized values of $\{n_{max} = 10$, $r_1 = 0.18$ GeV^{-1}, $r_{n_{max}} = 15$ GeV$^{-1}\}$ are finally selected for the heavy baryons in this work. Details can be found in Refs. [44, 45].

The set $\{\phi^G_{nlm}\}$ forms a set of finite-dimensional, non-orthogonal, and complete bases,

$$\begin{aligned}N_{n,n'} &= \langle\phi^G_{nlm}|\phi^G_{n'lm}\rangle = \left(\frac{2\sqrt{\nu_n\nu_{n'}}}{\nu_n+\nu_{n'}}\right)^{l+\frac{3}{2}},\\ 1 &= \sum_{n=1}^{n_{max}}\sum_{n'=1}^{n_{max}}|\phi^G_{nlm}\rangle(N^{-1})_{nn'}\langle\phi^G_{n'lm}|.\end{aligned} \tag{A3}$$

An arbitrary wave function $\psi_{lm}(\mathbf{r})$ can be expended in a set of definite orbital quantum states,

$$|\psi_{lm}\rangle = \sum_{n,n'=1}^{n_{max}}|\phi^G_{nlm}\rangle(N^{-1})_{nn'}\langle\phi^G_{n'lm}|\psi_{lm}\rangle \equiv \sum_{n=1}^{n_{max}}C_n|\phi^G_{nlm}\rangle. \tag{A4}$$

In the definite orbital quantum state, the matrix element of an operator $\hat{O}$ reads,

$$O_{nn'} = \langle\phi^G_{nlm}|\hat{O}|\phi^G_{n'lm}\rangle. \tag{A5}$$

Given $|(nlm)^G\rangle \equiv |n\rangle$ and $|(n'lm)^G\rangle \equiv |n'\rangle$, and operators $\hat{O}_1$, $\hat{O}_2$ and $\hat{O}_3$, the matrix element of their inner product in the set of bases is expressed as,

$$\begin{aligned}&\langle n|\hat{O}_1\hat{O}_2\hat{O}_3|n'\rangle\\ &= \sum_{\{n_i,n'_i\}}\langle n|\hat{O}_1|n_1\rangle(N^{-1})_{n_1n'_1}\langle n'_1|\hat{O}_2|n_2\rangle(N^{-1})_{n_2n'_2}\langle n'_2|\hat{O}_3|n'\rangle\\ &= \sum_{\{n_i,n'_i\}}(O_1)_{nn_1}(N^{-1})_{n_1n'_1}(O_2)_{n'_1n_2}(N^{-1})_{n_2n'_2}(O_3)_{n'_2n'}.\end{aligned} \tag{A6}$$

Here, $\sum_{\{n_i,n'_i\}}$ means sum over all the intermediate indices. The expectation value of an operator $\hat{O}$ in a state $|\alpha\rangle$ is written as,

$$\begin{aligned}\frac{\langle\alpha|\hat{O}|\alpha\rangle}{\langle\alpha|\alpha\rangle} &= \frac{\sum_{\{n\}}\langle\alpha|n^G_1\rangle(N^{-1})_{n_1n'_1}\langle n'_1|\hat{O}|n^G_2\rangle(N^{-1})_{n_2n'_2}\langle n'^G_2|\alpha\rangle}{\sum_{\{n\}}\langle\alpha|n^G_3\rangle(N^{-1})_{n_3n'_3}\langle n'^G_3|n^G_4\rangle(N^{-1})_{n_4n'_4}\langle n'^G_4|\alpha\rangle}\\ &= \frac{\sum_{\{n\}}C^*_{n'_1}O_{n'_1n_2}C_{n_2}}{\sum_{\{n\}}C^*_{n'_3}N_{n'_3n_4}C_{n_4}},\end{aligned} \tag{A7}$$

in the set of the Gaussian bases.

Now, given a definite quantum state $|(ls)_{JM_J}\rangle$, the generalized Gaussian basis function $(|[n,(ls)_{JM_J}]^G\rangle)$ is commonly written as

$$|[n,(ls)_{JM_J}]^G\rangle = \sum_{m_l,m_s}(lm_lsm_s|JM_J)\times|(nlm_l)^G\rangle\otimes|sm_s\rangle. \tag{A8}$$

The set $\{|[n,(ls)_{JM_J}]^G\rangle\}$ also forms a set of finite-dimensional, non-orthogonal, and complete bases,

$$\begin{aligned}N_{n,n'} &= \langle[n,(ls)_{JM_J}]^G|[n',(ls)_{JM_J}]^G\rangle = \left(\frac{2\sqrt{\nu_n\nu_{n'}}}{\nu_n+\nu_{n'}}\right)^{l+\frac{3}{2}},\\ 1 &= \sum_{n=1}^{n_{max}}\sum_{n'=1}^{n_{max}}|[n,(ls)_{JM_J}]^G\rangle(N^{-1})_{nn'}\langle[n',(ls)_{JM_J}]^G|.\end{aligned} \tag{A9}$$

For a singly heavy baryon, we introduce two independent sets of the Gaussian basis functions $|(n_\rho l_\rho m_\rho)^G\rangle$ and $|(n_\lambda l_\lambda m_\lambda)^G\rangle$ based on the JC-3 in Fig. 1. Given a definite quantum state $|\{[(l_\rho l_\lambda)_L(s_1s_2)_{s_{12}}]_j s_3\}_{JM_J}\rangle \equiv |\alpha\rangle_3$ (corresponding to the JC-3), the generalized Gaussian basis function has the form below,

$$\begin{aligned}|(\tilde{n},\alpha)^G_3\rangle = \sum_{\{m_\xi\}}\{CG_\xi\}\times&|(n_\rho l_\rho m_\rho)^G\rangle\otimes|(n_\lambda l_\lambda m_\lambda)^G\rangle\\ &\otimes|s_1m_{s_1}\rangle\otimes|s_2m_{s_2}\rangle\otimes|s_3m_{s_3}\rangle,\end{aligned} \tag{A10}$$

where $\{m_\xi\}$ denote all the 3rd components of the orbital

angular momenta and spins, $\{CG_\xi\}$ are the products of all the C-G coefficients. $\tilde{n}$ is obtained by combining n_ρ and n_λ, e.g., $\tilde{n}=(n_\rho-1)\times n_{max}+n_\lambda$ as $n_{\rho(\lambda)}=1,\cdots,n_{max}$.

The non-orthogonal and complete relations are as follows,

$$\begin{aligned} N_{\tilde{n},\tilde{n}'} &= \langle(\tilde{n},\alpha)_3^G|(\tilde{n}',\alpha)_3^G\rangle = \left(\frac{2\sqrt{\nu_{n_\rho}\nu_{n'_\rho}}}{\nu_{n_\rho}+\nu_{n'_\rho}}\right)^{l_\rho+\frac{3}{2}} \\ &\times\left(\frac{2\sqrt{\nu_{n_\lambda}\nu_{n'_\lambda}}}{\nu_{n_\lambda}+\nu_{n'_\lambda}}\right)^{l_\lambda+\frac{3}{2}}, \\ 1 &= \sum_{\tilde{n}=1}^{n_{max}^2}\sum_{\tilde{n}'=1}^{n_{max}^2}|(\tilde{n},\alpha)_3^G\rangle(N^{-1})_{\tilde{n}\tilde{n}'}\langle(\tilde{n}',\alpha)_3^G|. \end{aligned}$$

In the non-orthogonal representation of $|(\tilde{n}\alpha)_3^G\rangle$, the solution of the eigenenergy E belongs to a generalized matrix eigenvalue problem

$$\sum_{\tilde{n}'=1}^{n_{max}^2}(H_{\tilde{n}\tilde{n}'}-EN_{\tilde{n}\tilde{n}'})C_{\tilde{n}'}=0. \tag{A11}$$

The matrix element of an operator $\hat{H}$ reads,

$$\begin{aligned} H_{\tilde{n}\tilde{n}'} &= \langle(\tilde{n},\alpha)_3^G|\hat{H}|(\tilde{n}',\alpha)_3^G\rangle \\ &= \sum_{\{m_\xi\},\{m'_\xi\}}\{CG_\xi\}\times\{CG_{\xi'}\}\times\langle(n_\rho l_\rho m_\rho)^G|\langle(n_\lambda l_\lambda m_\lambda)^G| \\ &\times\langle s_1 m_{s_1}|\langle s_2 m_{s_2}|\langle s_3 m_{s_3}|\hat{H}|s_1 m'_{s_1}\rangle|s_2 m'_{s_2}\rangle|s_3 m'_{s_3}\rangle \\ &\times|(n'_\rho l_\rho m'_\rho)^G\rangle|(n'_\lambda l_\lambda m'_\lambda)^G\rangle \\ &\equiv \sum_{\{m_\xi,m'_\xi\}}\{CG_\xi\times CG_{\xi'}\}\times H_{(n_\rho n_\lambda,n'_\rho n'_\lambda);(m_{s_{1,2,3}},m'_{s_{1,2,3}})}. \end{aligned} \tag{A12}$$

The matrix element evaluation of $H_{\tilde{n}\tilde{n}'}$ is finally implemented for $H_{(n_\rho n_\lambda,n'_\rho n'_\lambda);(m_{s_{1,2,3}},m'_{s_{1,2,3}})}$. For the two-body interaction $\hat{V}_{ij}(r_{ij})$,

$$\begin{aligned} &[V_{ij}(r_{ij})]_{(n_\rho n_\lambda,n'_\rho n'_\lambda);(m_{s_{1,2,3}},m'_{s_{1,2,3}})} = [V(\rho_k)]_{(n_\rho n_\lambda,n'_\rho n'_\lambda);(m_{s_{1,2,3}},m'_{s_{1,2,3}})} \\ &\equiv\langle(n_{\rho_3} l_{\rho_3} m_{\rho_3})^G|\langle(n_{\lambda_3} l_{\lambda_3} m_{\lambda_3})^G| \\ &\times\langle s_1 m_{s_1}|\langle s_2 m_{s_2}|\langle s_3 m_{s_3}|\hat{V}(\rho_k)|s_1 m'_{s_1}\rangle|s_2 m'_{s_2}\rangle|s_3 m'_{s_3}\rangle \\ &\times|(n'_{\rho_3} l_{\rho_3} m'_{\rho_3})^G\rangle|(n'_{\lambda_3} l_{\lambda_3} m'_{\lambda_3})^G\rangle. \end{aligned} \tag{A13}$$

If the matrix element $[V(\rho_k)]_{(n_\rho n_\lambda,n'_\rho n'_\lambda);(m_{s_{1,2,3}},m'_{s_{1,2,3}})}$ is independent of the spin operator, it can be written further as $[V(\rho_k)]_{(n_\rho n_\lambda,n'_\rho n'_\lambda)}\delta_{m_{s1}m'_{s1}}\delta_{m_{s2}m'_{s2}}\delta_{m_{s3}m'_{s3}}$. The matrix element $[V(\rho_k)]_{(n_\rho n_\lambda,n'_\rho n'_\lambda)}$ can be calculated with the help of the Jacobi coordinates transformation $(\boldsymbol{\rho}_3,\boldsymbol{\lambda}_3)\rightarrow(\boldsymbol{\rho}_k,\boldsymbol{\lambda}_k)$ (k=1, 2, 3), but it will be very tedious in the framework of the GEM.

B. Infinitesimally-shifted Gaussian (ISG) basis functions

In the calculation of Hamiltonian matrix elements of three-body systems, particularly, when the Jacobi coordinates transformations are employed, integrations over all of the radial and angular coordinates become laborious even with the Gaussian basis functions. This process can be simplified by introducing the infinitesimally-shifted Gaussian (ISG) basis functions by

$$\begin{aligned} \phi_{nlm}^G &= N_{nl}r^l e^{-\nu_n r^2}Y_{lm}(\bar{\mathbf{r}}) \\ &= N_{nl}\lim_{\varepsilon\rightarrow 0}\frac{1}{(\nu_n\varepsilon)^l}\sum_{\tilde{k}=1}^{\tilde{k}_{max}}C_{lm,\tilde{k}}e^{-\nu_n(\mathbf{r}-\varepsilon\mathbf{D}_{lm,\tilde{k}})^2}, \end{aligned} \tag{B1}$$

where, $r^lY_{lm}(\bar{\mathbf{r}})$ is replaced by a set of coefficients $C_{lm,\tilde{k}}$ and vectors $\mathbf{D}_{lm,\tilde{k}}$. In this way, the Jacobi coordinates transformation just needs to be completed in the exponent section.

Considering an arbitrary matrix element $[V(\rho_k)]_{(n_\rho n_\lambda,n'_\rho n'_\lambda)}$, $V(\rho_k)$ is a scalar function of the radii ρ_k (k = 1, 2, 3, corresponding to the JC-1, -2, -3, respectively), and the orbital angular momenta (l_ρ,m_ρ), (l_λ,m_λ), (l'_ρ,m'_ρ), and (l'_λ,m'_λ) are defined under the JC-3 in Fig. 1. Using the infinitesimally-shifted Gaussian (ISG) basis functions, we obtain

$$\begin{aligned} &[V(\rho_k)]_{(n_\rho n_\lambda,n'_\rho n'_\lambda)} \\ &=\langle\phi^G_{n_{\rho_3}l_{\rho_3}m_{\rho_3}}\phi^G_{n_{\lambda_3}l_{\lambda_3}m_{\lambda_3}}|V(\rho_k)|\phi^G_{n'_{\rho_3}l'_{\rho_3}m'_{\rho_3}}\phi^G_{n'_{\lambda_3}l'_{\lambda_3}m'_{\lambda_3}}\rangle \\ &=\{N_{nl}\}\{\lim_{\varepsilon\rightarrow 0}\frac{1}{(\nu_n\varepsilon)^l}\}\sum_{\{\tilde{k}\}}\{C_{lm,\tilde{k}}\}\langle e^{-\nu_{n_\rho}(\boldsymbol{\rho}-\varepsilon_\rho\mathbf{D}_\rho)}e^{-\nu_{n_\lambda}(\boldsymbol{\lambda}-\varepsilon_\lambda\mathbf{D}_\lambda)}| \\ &V(\rho_k)|e^{-\nu_{n_{\rho'}}(\boldsymbol{\rho}-\varepsilon_{\rho'}\mathbf{D}_{\rho'})}e^{-\nu_{n_{\lambda'}}(\boldsymbol{\lambda}-\varepsilon_{\lambda'}\mathbf{D}_{\lambda'})}\rangle. \end{aligned} \tag{B2}$$

Here, $\{\cdots\}$ denotes the product of the contained elements. $\sum_{\{\tilde{k}\}}$ means sum over all the $\tilde{k}$ values.

For the final integral of Eq. (31), the following Jacobi coordinates transformations are performed,

$$\begin{aligned} \boldsymbol{\rho} &= \boldsymbol{\rho}(\boldsymbol{\rho}_k,\boldsymbol{\lambda}_k) \\ \boldsymbol{\lambda} &= \boldsymbol{\lambda}(\boldsymbol{\rho}_k,\boldsymbol{\lambda}_k) \\ d\boldsymbol{\rho}d\boldsymbol{\lambda} &= \|J\|d\boldsymbol{\rho}_k d\boldsymbol{\lambda}_k, \end{aligned} \tag{B3}$$

with $\boldsymbol{\rho}\equiv\boldsymbol{\rho}_3$, $\boldsymbol{\lambda}\equiv\boldsymbol{\lambda}_3$, and k = 1, 2, 3. Here $|J|$ is the Jacobian determinant. The detailed derivation can be found in Ref. [54].

With the help of the ISG basis functions, the matrix

elements of the Hamiltonian terms H_0, G'_{ij}, $\tilde{S}_{ij}$, $\tilde{H}^{tensor}_{ij}$, and $\tilde{H}^{c}_{ij}$ can be evaluated directly. The detailed results can be found in Ref. [44].

C. Spin-orbit terms

In Eq. (5) of Sec. IIA, the spin-orbit term $H^{SO(v)}_{ij}$ reads,

$$\begin{aligned}\tilde{H}^{so(v)}_{ij} &= \frac{\mathbf{s}_i\cdot(\mathbf{r}_{ij}\times\mathbf{p}_i)}{2m_i^2 r_{ij}}\frac{\partial\tilde{G}^{so(v)}_{ii}}{\partial r_{ij}} + \frac{\mathbf{s}_j\cdot(-\mathbf{r}_{ij}\times\mathbf{p}_j)}{2m_j^2 r_{ij}}\frac{\partial\tilde{G}^{so(v)}_{jj}}{\partial r_{ij}} + \\ &+ \frac{[\mathbf{s}_i\cdot(-\mathbf{r}_{ij}\times\mathbf{p}_j)+\mathbf{s}_j\cdot(\mathbf{r}_{ij}\times\mathbf{p}_i)]}{m_i m_j r_{ij}}\frac{\partial\tilde{G}^{so(v)}_{ij}}{\partial r_{ij}} \\ &\equiv \tilde{H}^{so(v)ii}_{ij} + \tilde{H}^{so(v)jj}_{ij} + \tilde{H}^{so(v)ij}_{ij}. \end{aligned} \tag{C1}$$

The Jacobi coordinates transformations are denoted as

$$\begin{aligned}\mathbf{r}_{ij} &= A_{rij}\boldsymbol{\rho} + B_{rij}\boldsymbol{\lambda}, \\ \mathbf{p}_i &= A_{pi}\mathbf{p}_\rho + B_{pi}\mathbf{p}_\lambda, \end{aligned} \tag{C2}$$

with $\boldsymbol{\rho}_3 \equiv \boldsymbol{\rho}$ and $\boldsymbol{\lambda}_3 \equiv \boldsymbol{\lambda}$. A_{rij}, B_{rij}, A_{pi} and B_{pi} can be obtained by Eq. (13). Then, the spin-orbit term can be expressed in terms of the Jacobi coordinates $\boldsymbol{\rho}$ and $\boldsymbol{\lambda}$, taking the first part of the spin-orbit term as an example,

$$\begin{aligned}\tilde{H}^{SO(v)ii}_{ij} = \frac{\partial\tilde{G}^{so(v)}_{ii}}{r_{ij}\partial r_{ij}}\Bigg[&\frac{A_{rij}A_{pi}}{2m_i^2}\boldsymbol{l}_\rho\cdot\mathbf{s}_i + \frac{B_{rij}B_{pi}}{2m_i^2}\boldsymbol{l}_\lambda\cdot\mathbf{s}_i \\ &+ \frac{A_{rij}B_{pi}}{2m_i^2}(\boldsymbol{\rho}\times\mathbf{p}_\lambda)\cdot\mathbf{s}_i + \frac{B_{rij}A_{pi}}{2m_i^2}(\boldsymbol{\lambda}\times\mathbf{p}_\rho)\cdot\mathbf{s}_i\Bigg]. \end{aligned} \tag{C3}$$

The terms proportional to $\boldsymbol{\lambda}\times\mathbf{p}_\rho$ or $\boldsymbol{\rho}\times\mathbf{p}_\lambda$ are the three-body spin-orbit potentials, which have no contributions to the current calculations. The reason lies in the following result. According to the Wigner-Eckhart theorem, in the derivation of the matrix elements $\langle(\tilde{n}\alpha)^G_3|\frac{\partial\tilde{G}^{so(v)}_{ii}}{r_{ij}\partial r_{ij}}(\boldsymbol{\rho}\times\mathbf{p}_\lambda)\cdot\mathbf{s}_i|(\tilde{n}'\alpha)^G_3\rangle$, a reduced matrix element $\langle l_\rho l_\lambda L||\frac{\partial\tilde{G}^{so(v)}_{ii}}{r_{ij}\partial r_{ij}}\boldsymbol{\rho}\times\mathbf{p}_\lambda||l_\rho l_\lambda L\rangle$ appears and has the following form,

$$\begin{aligned}&\langle l_\rho l_\lambda L||\frac{\partial\tilde{G}^{so(v)}_{ii}}{r_{ij}\partial r_{ij}}\boldsymbol{\rho}\times\mathbf{p}_\lambda||l_\rho l_\lambda L\rangle \\ &= \sqrt{3}(2L+1)X\begin{pmatrix} l_\rho & l_\lambda & L \\ 1 & 1 & 1 \\ l_\rho & l_\lambda & L\end{pmatrix}\langle l_\rho||\frac{\partial\tilde{G}^{so(v)}_{ii}}{r_{ij}\partial r_{ij}}\boldsymbol{\rho}||l_\rho\rangle\langle l_\lambda||\mathbf{p}_\lambda||l_\lambda\rangle, \end{aligned} \tag{C4}$$

where $X(\cdots)$ is a 9-j coefficient. $\frac{\partial\tilde{G}^{so(v)}_{ii}}{r_{ij}\partial r_{ij}}$, $\boldsymbol{\rho}$ and $\mathbf{p}_\lambda$ are the irreducible spherical tensors of rank 0, 1 and 1, respectively. The 9-j coefficient has an important property, i.e., the result is one factor $(-1)^{\sum l_i}$ more than the original value, if any two rows (or columns) are permuted. Here $\sum l_i$ means sum over all the 9 elements. So, $X(\cdots)$ ends up being zero in Eq. (36).

Hence, the matrix element of $\tilde{H}^{so(v)ii}_{ij}$ in a certain baryon state is expressed,

$$\begin{aligned}&\langle(\tilde{n},\alpha)^G_3|\tilde{H}^{SO(v)ii}_{ij}|(\tilde{n}',\alpha)^G_3\rangle \\ &= \langle(\tilde{n},\alpha)^G_3\left|\frac{\partial\tilde{G}^{so(v)}_{ii}}{r_{ij}\partial r_{ij}}\left[\frac{A_{rij}A_{pi}}{2m_i^2}\boldsymbol{l}_\rho\cdot\mathbf{s}_i + \frac{B_{rij}B_{pi}}{2m_i^2}\boldsymbol{l}_\lambda\cdot\mathbf{s}_i\right]\right|(\tilde{n}',\alpha)^G_3\rangle \\ &\equiv \sum_{\{m_\xi,m'_\xi\}}\{CG_\xi CG_{\xi'}\}\Big[(\tilde{H}^{SO(v)ii}_{ij(1)})_{(n_\rho n_\lambda,n'_\rho n'_\lambda);(m_{s_{1,2,3}},m'_{s_{1,2,3}})} \\ &\quad + (\tilde{H}^{SO(v)ii}_{ij(2)})_{(n_\rho n_\lambda,n'_\rho n'_\lambda);(m_{s_{1,2,3}},m'_{s_{1,2,3}})}\Big], \end{aligned} \tag{C5}$$

with

$$\begin{aligned}&(\tilde{H}^{SO(v)ii}_{ij(1)})_{(n_\rho n_\lambda,n'_\rho n'_\lambda);(m_{s_{1,2,3}},m'_{s_{1,2,3}})} \\ &= \left[\frac{\partial\tilde{G}^{so(v)}_{ii}}{r_{ij}\partial r_{ij}}\left(\frac{A_{rij}A_{pi}}{2m_i^2}\boldsymbol{l}_\rho\cdot\mathbf{s}_i\right)\right]_{(n_\rho n_\lambda,n'_\rho n'_\lambda);(m_{s_{1,2,3}},m'_{s_{1,2,3}})}. \end{aligned} \tag{C6}$$

The calculation of Eq. (38) is done in two steps. First, the algebraic calculation of $\mathbf{l}_\rho\cdot\mathbf{s}_i$ is performed,

$$\begin{aligned}&(\boldsymbol{l}_\rho\cdot\mathbf{s}_i)|s_1m'_{s_1}\rangle|s_2m'_{s_2}\rangle|s_3m'_{s_3}\rangle|(n'_\rho l_\rho m'_\rho)^G\rangle|(n'_\lambda l_\lambda m'_\lambda)^G\rangle \\ &= \sum_\kappa \xi_\kappa\times(|s_1m''_{s_1}\rangle|s_2m''_{s_2}\rangle|s_3m''_{s_3}\rangle|(n'_\rho l_\rho m''_\rho)^G\rangle|(n'_\lambda l_\lambda m''_\lambda)^G\rangle)_\kappa. \end{aligned} \tag{C7}$$

Second, the remaining part with $\frac{\partial\tilde{G}^{so(v)}_{ii}}{r_{ij}\partial r_{ij}}$ in Eq. (38) is finished by means of the ISG basis functions and the Jacobi coordinates transformation $(\boldsymbol{\rho}_3,\boldsymbol{\lambda}_3) \to (\boldsymbol{\rho}_k,\boldsymbol{\lambda}_k)$ (k=1,2,3). In this way, all the matrix elements of the spin-orbit terms can be computed rigorously.

D. Tables of the results

References

[1] F. Gross, E. Klempt, S. J. Brodsky, *et al.*, Eur.Phys.J.C **83**, 1125 (2023), arXiv: 2212.11107[hep-ph]
[2] S. Navas, *et al.*, Phys. Rev. D **110**(3), 030001 (2024)
[3] R. Mizuk, *et al.*, Phys. Rev. Lett. **94**, 122002 (2005), arXiv: hep-ex/0412069[hep-ex]
[4] B. Aubert, *et al.*, Phys. Rev. D **77**, 012002 (2008), arXiv: 0710.5763[hep-ex]
[5] B. Aubert, *et al.*, Phys. Rev. D **78**, 112003 (2008), arXiv: 0807.4974[hep-ex]
[6] R. Aaij, *et al.*, JHEP **05**, 030 (2017), arXiv: 1701.07873[hep-ex]
[7] R. Aaij, *et al.*, Phys. Rev. Lett. **118**(18), 182001 (2017), arXiv: 1703.04639[hep-ex]
[8] J. Yelton, *et al.*, Phys. Rev. D **97**(5), 051102 (2018), arXiv: 1711.07927[hep-ex]
[9] Y. B. Li, *et al.*, Eur. Phys. J. C **78**(3), 252 (2018), arXiv: 1712.03612[hep-ex]
[10] R. Aaij, *et al.*, Phys. Rev. Lett. **121**(7), 072002 (2018), arXiv: 1805.09418[hep-ex]
[11] Y. B. Li, *et al.*, Eur. Phys. J. C **78**, 928 (2018), arXiv: 1806.09182[hep-ex]
[12] R. Aaij, *et al.*, Phys. Rev. Lett. **122**(1), 012001 (2019), arXiv: 1809.07752[hep-ex]
[13] R. Aaij, *et al.*, Phys. Rev. Lett. **124**(8), 082002 (2020), arXiv: 2001.00851[hep-ex]
[14] R. Aaij, *et al.*, Phys. Rev. Lett. **124**, 222001 (2020), arXiv: 2003.13649[hep-ex]
[15] R. Aaij, *et al.*, Phys. Rev. Lett. **103**(1), 012004 (2021), arXiv: 2010.14485[hep-ex]
[16] R. Aaij, *et al.*, Phys. Rev. D **104**(9), L091102 (2021), arXiv: 2107.03419[hep-ex]
[17] Y. B. Li, *et al.*, Phys. Rev. Lett. **130**(3), 031901 (2023), arXiv: 2206.08822[hep-ex]
[18] R. Aaij, *et al.*, Phys. Rev. D **108**, 012020 (2023), arXiv: 2211.00812[hep-ex]
[19] R. Aaij, *et al.*, Phys. Rev. Lett. **131**(13), 131902 (2023), arXiv: 2302.04733[hep-ex]
[20] R. Aaij, *et al.*, Phys. Rev. Lett. **131**(17), 171901 (2023), arXiv: 2307.13399[hep-ex]
[21] R. Aaij *et al.* (LHCb Collaboration), arXiv: 2409.05440[hep-ex].
[22] R. Aaij *et al.* (LHCb Collaboration), arXiv: 2502.18987[hep-ex].
[23] H. Y. Cheng, Chin. J. Phys. **78**, 324 (2022), arXiv: 2109.01216[hep-ph]
[24] H. X. Chen, W. Chen, X. Liu, *et al.*, Rept. Prog. Phys. **86**(2), 026201 (2023), arXiv: 2204.02649[hep-ph]
[25] V. Crede and J. Yelton, Rept. Prog. Phys. **87**(10), 106301 (2024)
[26] S. Godfrey and N. Isgur, Phys. Rev. D **32**, 189 (1985)
[27] S. Capstick and N. Isgur, Phys. Rev. D **34**, 2809 (1986)
[28] X. Z. Weng, W. Z. Deng and S. L. Zhu, Phys. Rev. D **110**(5), 056052 (2024), arXiv: 2405.19039[hep-ph]
[29] S. Capstick and W. Roberts, Prog. Part. Nucl. Phys. **45**, S241 (2000), arXiv: nucl-th/0008028[nucl-th]
[30] N. Isgur and M. B. Wise, Phys. Rev. Lett. **66**, 1130 (1991)
[31] H. Georgi, Phys. Lett. B **240**, 447 (1990)
[32] E. Eichten and B. R. Hill, Phys. Lett. B **234**, 511 (1990)
[33] W. Roberts and M. Pervin, Int. J. Mod. Phys. A **23**, 2817 (2008), arXiv: 0711.2492[nucl-th]
[34] D. Ebert, R. N. Faustov and V. O. Galkin, Phys. Rev. D **84**, 014025 (2011), arXiv: 1105.0583[hep-ph]
[35] J. R. Zhang, Phys. Rev. D **89**(9), 096006 (2014), arXiv: 1212.5325[hep-ph]
[36] H. Y. Cheng, arXiv: 1508.07233[hep-ph].
[37] H. X. Huang, J. L. Ping and F. Wang, Phys. Rev. D **97**(3), 034027 (2018), arXiv: 1704.01421[hep-ph]
[38] Z. G. Wang, Nucl. Phys. B **926**, 467 (2018), arXiv: 1705.07745[hep-ph]
[39] Q. F. Lü and X. H. Zhong, Phys. Rev. D **101**(7), 014017 (2020), arXiv: 1910.06126[hep-ph]
[40] Z. G. Wang and H. J. Wang, Chin. Phys. C **45**(1), 013109 (2021), arXiv: 2006.16776[hep-ph]
[41] A. Kakadiya, Z. Shah and A. K. Rai, Int. J. Mod. Phys. A **37**(11n12), 2250053 (2022), arXiv: 2202.12048[hep-ph]
[42] Q. Xin, Z. G. Wang and F. Lü, Chin. Phys. C **47**, 093106 (2023), arXiv: 2306.05626[hep-ph]
[43] E. Ortiz-Pacheco and R. Bijker, Phys. Rev. D **108**(5), 054014 (2023), arXiv: 2307.04939[hep-ph]
[44] G. L. Yu, Z. Y. Li, Z. G. Wang, *et al.*, Nucl. Phys. B **990**, 116183 (2023), arXiv: 2206.08128[hep-ph]
[45] Z. Y. Li, G. L. Yu, Z. G. Wang, *et al.*, Chin. Phys. C **47**, 073105 (2023), arXiv: 2207.04167[hep-ph]
[46] G. L. Yu, Z. Y. Li, Z. G. Wang, *et al.*, Eur. Phys. J. A **59**, 126 (2023), arXiv: 2211.00510[hep-ph]
[47] Z. Y. Li, G. L. Yu, Z. G. Wang, *et al.*, Mod. Phys. Lett. A **38**(08n09), 2350052 (2023), arXiv: 2210.13085[hep-ph]
[48] Z. Y. Li, G. L. Yu, Z. G. Wang, *et al.*, Int. J. Mod. Phys. A **38**(18n19), 2350095 (2023), arXiv: 2211.15111[hep-ph]
[49] Z. Y. Li, G. L. Yu, Z. G. Wang, *et al.*, Eur. Phys. J. C **84**(2), 106 (2024), arXiv: 2311.08251[hep-ph]
[50] Z. Y. Li, G. L. Yu, Z. G. Wang, *et al.*, Eur. Phys. J. C **84**(12), 1310 (2024), arXiv: 2405.16162[hep-ph]
[51] N. Isgur and G. Karl, Phys. Rev. D **18**, 4187 (1978)
[52] N. Isgur, Phys. Rev. D **62**, 014025 (2000), arXiv: hep-ph/9910272[hep-ph]
[53] M. Kamimura, Phys. Rev. A **38**, 621 (1988)
[54] E. Hiyama, Y. Kino and M. Kamimura, Prog. Part. Nucl. Phys. **51**, 223 (2003)
[55] Q. F. Lü, D. Y. Chen and Y. B. Dong, Phys. Rev. D **102**, 034012 (2020), arXiv: 2006.08087[hep-ph]
[56] H. H. Zhong, M. S. Liu, R. H. Ni, *et al.*, Phys. Rev. D **110**(11), 116034 (2024), arXiv: 2409.07998[hep-ph]
[57] Z. L. Zhang, Z. W. Liu, S. Q. Luo, *et al.*, Phys. Rev. D **107**(3), 034036 (2023), arXiv: 2210.17188[hep-ph]
[58] B. Chen, S. Q. Luo and X. Liu, Eur. Phys. J. C **81**(5), 474 (2021), arXiv: 2101.10806[hep-ph]